Received: 11 July 2022 | Revised: 9 October 2022 | Accepted: 29 November 2022

DOI: 10.1111/1541-4337.13095

COMPREHENSIVE REVIEW

Comprehensive REVIEWS in Food Science and Food Safety WILEY

Metal–oxide–semiconductor resistive gas sensors for fish freshness detection

Kaidi Wu[1,2] | **Marc Debliquy**[2] | **Chao Zhang**[1]

[1]College of Mechanical Engineering, Yangzhou University, Yangzhou, China

[2]Service de Science des Matériaux, Faculté Polytechnique, Université de Mons, Mons, Belgium

Correspondence
Chao Zhang, College of Mechanical Engineering, Yangzhou University, Huayang West Road 196, Yangzhou, Jiangsu, 225127, China.
Email: zhangc@yzu.edu.cn

Funding information
Outstanding Youth Foundation of Jiangsu Province of China, Grant/Award Number: BK20211548; National Natural Science Foundation of China, Grant/Award Number: 51872254; Excellent Doctoral Dissertation Fund of Yangzhou University, Grant/Award Number: 2021_06; National Key Research and Development Program of China, Grant/Award Number: 2017YFE0115900

Abstract

Fish are prone to spoilage and deterioration during processing, storage, or transportation. Therefore, there is a need for rapid and efficient techniques to detect and evaluate fish freshness during different periods or conditions. Gas sensors are increasingly important in the qualitative and quantitative evaluation of high-protein foods, including fish. Among them, metal–oxide–semiconductor resistive (MOSR) sensors with advantages such as low cost, small size, easy integration, and high sensitivity have been extensively studied in the past few years, which gradually show promising practical application prospects. Herein, we take the detection, classification, and assessment of fish freshness as the actual demand, and summarize the physical and chemical changes of fish during the spoilage process, the volatile marker gases released, and their production mechanisms. Then, we introduce the advantages, performance parameters, and working principles of gas sensors, and summarize the MOSR gas sensors aimed at detecting different kinds of volatile marker gases of fish spoiling in the last 5 years. After that, this paper reviews the research and application progress of MOSR gas sensor arrays and electronic nose technology for various odor indicators and fish freshness detection. Finally, this review points out the multifaceted challenges (sampling system, sensing module, and pattern recognition technology) faced by the rapid detection technology of fish freshness based on metal oxide gas sensors, and the potential solutions and development directions are proposed from the view of multidisciplinary intersection.

KEYWORDS
electronic nose, fish freshness, metal oxides, nondestructive detection, semiconductor gas sensors

1 | INTRODUCTION

With the rapid economic development and the improvement of people's life quality, issues such as the freshness and safety quality of agricultural products have received extensive attention. Fish is extremely nutritious; rich in protein, amino acids, vitamins, and minerals; and is a source of nutrients necessary for people's health. Fish-related industries are also an important part of the world's economy (Weichselbaum et al., 2013). In addition, the rapid development of transportation and storage technology enables high-quality fish and its processed products to reach all parts of the world. According to statistics, the fisheries and aquaculture industry provides at least 220 million tons of fish annually to the world. The demand for fish and related products is still increasing dramatically

(Waite & Beveridge, 2014). However, the biggest challenge in meeting the needs of all is the perishability of fish (Ghaly et al., 2010). Compared with other meats, fish will produce various metabolites that lead to their deterioration after fishing, and the muscle tissue of fish will be changed (first hardening then softening) (Wu, Pu, et al., 2019). In addition, fish is rich in psychrophilic microorganisms, which can also reproduce under refrigeration conditions (Cheng et al., 2014). At the same time, due to the action of enzymes and the oxidation of their fat, fish and fish products are easily corrupted and deteriorated during processing, storage, or transportation. It not only decomposes their nutrients and reduces their nutritional value, but also produces toxic and harmful substances. Various fishy smell gases affect food safety, quality, and even human health (Hassoun & Karoui, 2017; Wu, Zhang, et al., 2021). In conclusion, there is a need for fast and efficient methods to detect and evaluate the freshness of fish and fish products during different periods or conditions (Johnson et al., 2019; Prabhakar et al., 2020).

In general, the changes in microorganisms, physical and chemical reactions, flavor substances, body surface color, and microbial colonies will occur during the fish spoilage process, which can be used as the physical and chemical indicators (Bernardo et al., 2020). Hence, physical and chemical experimental analysis and sensory evaluation methods are applied to detect the fish freshness (Cheng et al., 2015; Prabhakar et al., 2020). As for physical and chemical analysis, gas chromatography (GC), high-performance liquid chromatography (HPLC), and gas chromatography–mass spectrometry (GC–MS) are used to determine the fish quality indicators, such as total volatile basic nitrogen (TVB-N), *K* value, pH value, microbial colonies and their total viable counts (TVC), and biological ammonia (NH_3). Although these methods are accurate in evaluating freshness, they have the limitations of high cost, complicated instrument operation, long detection cycle, and low degree of automation (Cheng et al., 2013; Jia et al., 2018). As for the sensory evaluation methods, professional evaluators assess the color, smell, taste, and tissue morphology of the fish according to national standards, and finally summarize the more subjective quality level (Huang et al., 2021). The abovementioned traditional detection methods are all destructive testing, which is also limited by experimental hardware and software conditions and professional level of evaluators. Therefore, accurate and nondestructive detection methods are demanded to supplement or replace traditional detection techniques (Wu, Pu, et al., 2019). Several nondestructive detection techniques have been increasingly applied in the field of food safety, including near-infrared spectroscopy (NIRS), hyperspectral imaging, multispectral imaging (MSI), nuclear magnetic resonance (NMR), and machine vision (MV) (Kutsanedzie et al., 2019; Zaukuu et al., 2020). However, NIRS can only cover a small sample surface, leading to low spectral size data and only predicting some of its chemical properties (Kademi et al., 2019). MSI has a very narrow range of predictable quality attributes due to the utility of only a few spectral images of interest (Kutsanedzie et al., 2019). The detection reliability of NMR and MV is only improved when the detection object is homogeneous or nearly homogeneous (Hassoun & Karoui, 2017). Hence, the limitations mentioned above make them unsuitable for real-time assessment of product quality from a consumer's perspective or on spot.

The deterioration of fish freshness during storage or processing will affect their color, texture, and odor. Notably, odor quality is one of the most important factors affecting consumer buying behavior (Jiang & Liu, 2020). Therefore, the detection and evaluation of odor indicators will be a nondestructive testing method. The gas sensors have attracted attention in the last decade, which can be defined as the device able to transform the unpredictable information in an analytically useful signal. The gas sensors based on various working principles can be classified as metal–oxide–semiconductor (MOS) gas sensor, catalytic combustion gas sensor, electrochemical gas sensor, optical gas sensor, and surface acoustic wave gas sensor. In the current research, metal–oxide–semiconductor resistive (MOSR) gas sensors with low cost, easy integration, high sensitivity, and easy operation have become an emerging rapid nondestructive assessment method. The mainstream sensing mechanism of MOSR gas sensor is based on the chemical or physical adsorption/desorption of the gas molecules on the material surface, resulting in a change in resistance due to the change in charge carrier concentration. The detection technique based MOSR gas sensors has been widely applied to detect the odor indicators of food. Olafsson et al. used a metal oxide sensor to detect the freshness of cod in frozen storage. As the concentration of volatile gas in the fish increased, the sensor response changed linearly, and this method could detect the early spoilage of the fish (Ólafsson et al., 1992). Schweizer-Berberich et al. (1994) utilized eight sensors to detect odor changes in refrigerated trout and found a good correlation between sensor responses and amines and sulfides in fish volatile gases. Hammond et al. (2002) studied the freshness of Atlantic frogs and Atlantic crocodiles using gas sensor arrays and headspace methods. They found that sensor signals correlated well with sensory evaluation, pH, trimethylamine (TMA), total bacteria, and TVB-N. Kent et al. (2004) used nine field-effect and six MOS sensors to measure fish freshness and used the principal component analysis (PCA) method to identify fish freshness. The above work proves MOS gas sensing technology is

a rapid, low-cost, and nondestructive freshness detection technology.

With the increasing demand for high nutrients such as fish and the impact of long-distance cold chain logistics, it is urgent to develop a fast, accurate, easy-to-operate, and even online application of fish odor quality detection technology. For this goal, MOSR gas sensor technology has developed rapidly in recent years (Galstyan et al., 2018; Pereira et al., 2021). Though the MOS-based gas sensors were discussed in several reported reviews, these reviews only briefly introduced the gas sensors toward limited target gases and the corresponding electronic noses. Additionally, the current research state and application progress of MOSR gas sensors are rarely focused and discussed systematically in the reported reviews. This review first summarized the types, concentration levels, and generation principles of volatile compounds released from the fish spoilage process, and the working principle of MOSR gas sensors was introduced. Then, the research and application progress of MOSR gas sensors (arrays) and electronic nose technology with single odor or multiple odors as indicators were reviewed separately. Finally, the various challenges faced by this technology were pointed out, and the corresponding possible solutions were proposed, including the development of new gas-sensing materials, the common applicability of semiconductor gas sensors and wireless communication technologies, the improvement of pattern recognition algorithms and device structures, the simplified use of high-performance semiconductor gas sensors in fish quality monitoring, and so forth.

2 | VOLATILE GAS ANALYSIS DURING FISH SPOILAGE AND WORKING PRINCIPLE OF MOSR GAS SENSORS

2.1 | Volatile gas analysis during fish spoilage

Fish is nutritious and essentially healthy food. But compared to other livestock meat, fish is more prone to spoilage. The structure of fish and environmental factors are the main reasons: unsaturated fatty acids in fish are more easily oxidized than saturated fatty acids in poultry and livestock meat; the soluble protein in fish that is easily absorbed by the human body also provides sufficient nutrition for the growth and reproduction of microorganisms; the lack of dense connective tissue and fascia makes it easy for bacteria in the fish epidermis to spread from the outside to the inside; the content of endogenous enzymes in aquatic products, including fish, is higher than that in other meats; and higher ambient temperature will enhance the activity of endogenous enzymes, promote the change and decomposition of fish tissue, and create a favorable external environment for bacterial growth (Miyasaki et al., 2011; Olafsdóttir et al., 1997; Pei et al., 2021; Pons-Sánchez-Cascado et al., 2005).

As a result, freshness is highly variable during the storage or transport of fish, from fresh to flat, sweet, stale, and eventually spoiled or stinky. And the odors will originate from different volatile compounds. On the one hand, the odor of fresh fish originates from low concentrations (ppb) of volatile compounds derived from the oxidation of long-chain polyunsaturated fatty acids (Han et al., 2014; Zhuang et al., 2021). On the other hand, the odors of rotten fish, such as fishy, bad, or putrid smell, are mainly ascribed to the release of higher concentrations of amines, H_2S, aldehydes, alcohols, and ketones (the decomposition of amino acids, fatty acids, and carbohydrates under the action of microorganisms and enzymes) (Kent et al., 2004; Olafsdottir et al., 2004). In detail, trimethylamine oxide (TMAO) of sea fish is reduced into TMA and dimethylamine (DMA) by the reaction of enzymes, which is the major cause of the fishy smell. However, TMA is not recommended as an indicator of freshness for freshwater fish due to the less TMAO in vivo. Therefore, two chemical attributes are used for freshwater fish, including TVB-N and biogenic amines (Wu, Pu, et al., 2019). Hydrogen sulfide is derived from the degradation of proteins by specific spoilage organisms (*Pseudomonas*, *Shewanella*). Among them, *S*hewanella *baltica* is considered to be the main bacteria for producing H_2S in deep-sea fish, which will generate specific signaling products to promote a possible spoilage process (Gu et al., 2013). The unsaturated fatty acids are decomposed into ketones and aldehydes, and carbohydrates are decomposed into alcohols, ketones, and so forth. Table 1 summarizes the types of gases and volatile organic compounds detected in rotten fish and their biochemical generation mechanisms. In addition, the means of food spoilage and the release of volatile organic compounds during spoilage depend on the fish species (e.g., deep-sea fish, freshwater fish).

2.2 | Working principle of MOSR gas sensors

Taking the volatile organic compounds from fish as target gases is a rapid and effective way to realize freshness assessment and control fish quality using gas sensors with low cost, real-time monitoring, and high sensitivity. With the development of bionic olfactory system and gas sensing technology, gas sensors that detecting released gases such as amines, ammonia, alcohols, and sulfur-containing odors produced during the spoilage process of

TABLE 1 The volatile gas or organic compounds during the fish spoilage process (Duflos et al., 2006; Heising et al., 2014; Katiyo et al., 2020; Li, Zhang, et al., 2018; Olafsdóttir et al., 1997; Parlapani et al., 2017; Pei et al., 2021)

Group	Volatile compounds	Biochemical mechanism
Amine	Ammonia (NH_3) Monomethylamine (MMA) Dimethylamine (DMA) Trimethylamine (TMA) Triethylamine (TEA)	Deamination of amino acids or catabolism of trimethyl alkyl compounds
Sulfides	Hydrogen sulfide (H_2S) Dimethyl sulfide (DMS) Dimethyl disulfide (DMDS)	Catabolism of sulfur-containing amino acids (methionine and cysteine)
Alcohols	Ethanol Methyl mercaptan Ethanethiol	Proteolytic activity of amino acids metabolism, methyl ketone reduction, aldehydes reduction
Ketones	Acetone 3-Pentanone	Lipolytic activity or bacterial dehydrogenation of alcohols and degradation of alkanes
Aldehydes	Acetaldehyde Methyl-butanal	Hydrolysis of triglycerides, oxidation of fatty acids, transamination of amino acids

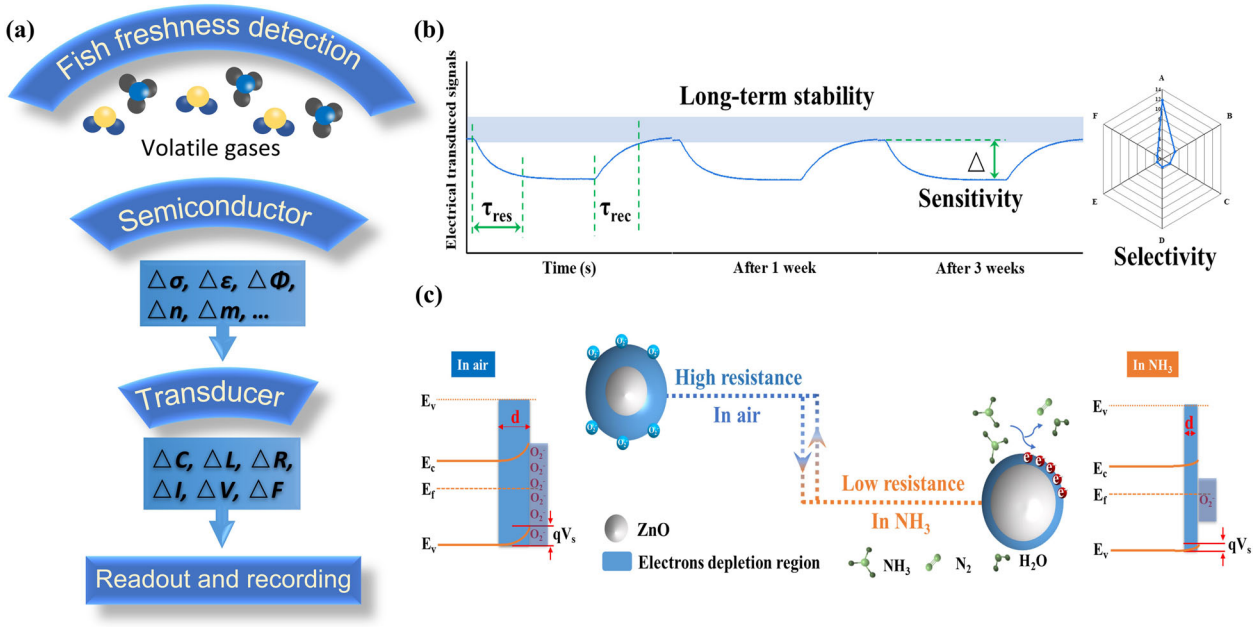

FIGURE 1 (a) Semiconductor gas sensors based on different signal conversion mechanisms. *M*, mass; *σ*, conductivity; *Φ*, work function; *n*, refractive index; *ε*, permittivity; *C*, capacitance; *L*, inductance; *R*, resistance; *I*, current; *V*, voltage; *F*, frequency. (b) Performance parameters of metal oxide gas sensors. (c) Schematical diagram of sensing mechanism of metal oxide gas sensors (taking n-type ZnO for detecting reducing NH_3 gas as an example)

fish come into being. In Figure 1a, the gas sensor converts the reaction of different odor molecules (such as NH_3, H_2S, triethylamine [TMA], etc.) on its surface into measurable physical/electrical signals and obtains the type and concentration of the gas to be detected according to the signal characteristics, to achieve rapid detection of freshness, easy operation, and good repeatability.

The design of gas sensor is commonly based on gas-sensitive material and signal transducer. The sensitive materials include metal oxides, layered two-dimensional nanomaterials (such as graphene, transition metal dichalcogenides, hexagonal boron nitride, etc.), organic semiconductors, and biological materials. Many gas sensors have been developed to meet the requirements

of practical applications and show excellent application potential. According to the signal conversion mechanism (Figure 1a), gas sensors can be divided into physical, chemical, and biological sensors. Among them, chemical gas sensors are widely used, mainly including optical signals (infrared sensors), mass signals (quartz crystal microbalance QCM sensor), and electrical signals (chemiresistive, impedance, field-effect transistor, electrochemical and capacitive sensors, etc.) (Huan et al., 2020; Semeano et al., 2018; Verma & Yadava, 2015; Yuan et al., 2020, 2022; Zhang, Li, et al., 2022). Among them, MOSR gas sensors have attracted wide attention and has become a research hotspot in many fields, including food quality monitoring.

The performance parameters of MOSR gas sensor are shown in Figure 1b, mainly response (R_a/R_g for reducing gases and R_g/R_a for oxidizing gases, where R_a is the resistance of the gas sensor in the reference gas [commonly air] and R_g is the resistance in the target gas), response/recovery time (the time required for achieving 90% of the resistance values change [$\triangle R$] when the exposed gas changed), selectivity (the ability of the gas sensors to detect a specific gas in a mixture of gases), repeatability (the ability of the gas sensors return to their original state when gas concentration returns to normal), and long-term operation stability (the ability of the gas sensors to keep a stable response working for a long term) (Li et al., 2021; Wu, Li, et al., 2019; Zhang, Huan, et al., 2022). The mainstream gas-sensing mechanism of resistive-type MOS gas sensor is shown in Figure 1c (using n-type ZnO as the gas-sensing material and reducing NH_3 as the target gas) (Feng, Wu, Chen, et al., 2022; Wang, Yang, et al., 2021). When the gas sensor is exposed to air, as the electron affinity of oxygen is higher, the free electrons of the conduction band will be transferred to the surface, and adsorbed oxygen ions (O_2^-, O^-, O^{2-}) are generated. At the same time, the energy bands bend upward (Schottky barrier height), forming an electron depletion region (EDR) at the interface, thus leading to the high resistance of the gas sensor. When the gas sensor is exposed to the target gas, the occurred redox reaction ($4NH_3 + 3O_2^-$ [ads] $\rightarrow 2N_2 + 6H_2O + 3e^-$) will release electrons back into the metal oxide and reduce the Schottky barrier height, making the EDR thinner and decreasing the resistance of gas sensor. After this process undergoes many cycles, insufficient desorption, low diffusion efficiency, and other processes may occur, thus ending the lifetime of the gas sensor. To achieve advanced improvements in both selectivity and sensitivity at optimal working temperature, the different configurations of MOS often stem from electronic structure and charge distribution, such as designing and constructing nanomaterials with special morphology and nanostructure, inducing defected state, and introducing the secondary phase (highly tunable composition, increasing semiconductor junction, and creating larger electron depletion) (Feng, Wu, Ren, et al., 2022; Wang, Yang, et al., 2021).

3 | GAS SENSORS FOR SINGLE ODOR

Gas sensors can identify some of the gases emitted by spoiled food. Rapid, qualitative, and quantitative detection of the released gases from fish spoilage through gas sensors is useful and practical in fish freshness evaluation. Therefore, it is important to choose a suitable sensor to detect specific gases in spoiled fish. This section will summarize the research and application progress of single-odor gas sensors in the past 5 years.

3.1 | Trimethylamine

Various odors are released during the spoilage process of sea fish, among which TMA gas is a major volatile organic compound. TMAO acts as an osmoregulatory factor to reduce dehydration along with the issue of waterlogging in the freshwater fish tissues. Several bacteria such as *Aeromonas* spp., *Photobacterium phosphoreum*, *Enterobacteriaceae*, and *Vibrio* spp. reduce TMAO to TMA to obtain energy after which the creation of ammonia-like off-flavors takes place (Ghaly et al., 2010; Prabhakar et al., 2020). Hence, fresh seafood contains small amounts of TMA, but high amounts of tasteless TMAO (e.g., olive flounder: 4.1 mmol/L, red halibut: 5.3 mmol/L, etc.) (Mitsubayashi et al., 2004). The reduction of TMAO by microorganisms will produce TMA, whose concentration will increase rapidly after seafood dies. The Food and Agriculture Organization of the United Nations reports that good-quality cold-water fish contains less than 6.3 mg/100 g (63 ppm) of TMA (Nevigato et al., 2018). The maximum reference TMA content cited by the Italian Istituto Zooprofilattico Sperimentale (IZSUM, Ministry of Health) for the freshness of marine fish was less than 5.0 mg/100 g (50 ppm) of TMA (Haouet, 2001; Nevigato et al., 2018). The TMA measurement in seafood has been reported to be one of the indicators for the evaluation of fish freshness by Japanese scientists (fresh: 0–1 mg/100 g, <10 ppm; initial corruption: 1–5 mg/100 g, 10–50 ppm; rotting fish [uneatable in the raw]: >6 mg/100 g, >60 ppm) (Mitsubayashi et al., 2004). Hence, the freshness can be evaluated using the released TMA concentration. It also guides the design and performance indicators of MOSR gas sensors according to the fish origin and species.

Molybdenum trioxide (MoO_3) is a common acidic oxide, which shows a good detection effect on basic TMA. Li et al. designed a TMA gas sensor based on n-type MoO_3

nanoribbons. At 280°C, the response value to 10 ppm TMA was 10.2, but its linear detection range and selectivity needed further improvement. The research group used p-type $CoMoO_4$ as the reinforcing phase to form a $CoMoO_4/MoO_3$ heterojunction composite gas sensor. Compared with pure MoO_3, the working temperature of the $CoMoO_4/MoO_3$ was reduced to 220°C, the response to 10 ppm TMA was increased to 25.2, and the response time was shortened to 10 s, and the linear response range is 5–100 ppm. It also showed good selectivity and stability (Li, Song, et al., 2018). The strong oxygen adsorption capacity of p-type $CoMoO_4$, the surface defects of the crystal, and the p–n heterojunction at the interface of the composite material effectively improve the charge transfer rate and redox reaction efficiency of the gas-sensing layer, thereby greatly enhancing the sensing properties. In addition, Zhang et al. developed a hollow and heterojunction structure composite based on $MoO_3/Bi_2Mo_3O_{12}$ and applied it as a TMA sensor for the first time. High response (7.2 at 10 ppm), good linear detection range (0.1–100 ppm), humidity resistance, and selectivity make it one of the candidates for detecting seafood freshness (Zhang et al., 2019). To further reduce the operating temperature of the sensor, Shen et al. developed a TMA gas sensor based on rich-oxygen vacancy and porous α-MoO_3 nanosheets, which exhibited a good linear response to 0.02–50 ppm TMA at 133°C, with a detection limit of up to 20 ppb. Its cyclability was verified, and the response value to a specific concentration of TMA was stable within 3 months, showing great potential for practical applications (Shen et al., 2019).

In addition, Fe_2O_3 with various morphologies also showed application value in the field of TMA detection. Wang et al. synthesized α-Fe_2O_3 mesoporous nanorod arrays by an ionic liquid-assisted hydrothermal method (Wang et al., 2017). Because of the mesoporous structure, large specific surface area, and the functionalized ionic liquid, the α-Fe_2O_3 nanorod array obtained the facilitated adsorption/diffusion of TMA molecules on the surface and enhanced electron transfer efficiency, thus attaining excellent gas-sensing performance. The sensor exhibited high response, fast recovery, and good cyclability toward TMA, and a fine linear response in the concentration range of 0.1–100 ppm, which will contribute to quantitative analysis (Figure 2a,b). The research group first used the α-Fe_2O_3 sensor to rapidly analyze the freshness changes of crucian carp (100 g) stored at 0 and 25°C. As shown in Figure 2c, the response also showed a positive linear relationship with the fish storage time (R^2 = .9860, R^2 = .9878) from 0 to 11 h. When the sensor detected fish stored at 25°C for 0 and 11 h, the response values were 4.4 and 12.7, and the response/recovery times were 5/1 s and 50/159 s, respectively. Additionally, the sensor showed higher response to crucian carp (100 g) stored at 25°C, indicating the fish is more prone to spoilage at room temperature. Furthermore, the gas chromatogram result of fish spoilage volatiles after storage at 25°C for 0–11 h (Figure 2c) indicated that the major volatile is TMA. In addition, the intensity of these peaks gradually increased, clearly indicating that the amount of TMA increased with the deterioration of fish freshness. This trend is also consistent with the sensor's response to different concentrations of TMA released during crucian carp spoilage. Therefore, the α-Fe_2O_3 mesoporous nanorod array thin film sensor can monitor the spoilage volatiles gas of crucian carp in real time. Shen et al. designed and fabricated bimetallic (Au@Pt) modified α-Fe_2O_3 hollow nanocubes as a sensing material to detect TMA (Figure 2d) (Shen et al., 2021). α-Fe_2O_3 presents a unique hollow cubic structure, and Au@Pt is uniformly dispersed on the cube's surface. The homemade test system was used for sensor tests (Figure 2d). Benefiting from the large specific surface area and porous nature of the hollow cubes, the spillover effect of Au@Pt on α-Fe_2O_3 nanocubes and its synergistic catalysis on TMA, 1.0 wt%. The Au@Pt/α-Fe_2O_3 sensor exhibited significantly improved TMA gas-sensing performance at 150°C, high response (32 at 100 ppm TMA), fast response speed (5 s), low detection limit (1 ppm), and good selectivity. The gas-sensing mechanism based on hollow cubic structure and Au@Pt noble decoration was also elucidated (Figure 2e). The practicality of the Au@Pt/α-Fe_2O_3 was verified through detecting the TMA gas released from large yellow croaker (500 g) at different storage temperatures. In Figure 2f, the response values gradually increased with the storage time. When the storage time exceeded 7 days (5°C) and 3 days (25°C), the response value reached 10, indicating that the large yellow croaker had undergone severe spoilage. This evaluation result was also verified by GC–MS testing. Therefore, this work will provide guidance for rapid, portable, and nondestructive testing of fish freshness.

Tungsten trioxide (WO_3) also shows great sensing properties to TMA. Zhao et al. designed an ultraefficient TMA gas sensor based on Au nanoparticles-sensitized WO_3 nanosheets (Zhao et al., 2022). The Au/WO_3 sensor showed good sensing properties to TMA at 300°C, including the high response to 25 ppm TMA (R_a/R_g = 217.72), short response/recovery time (8/6 s), low detection limit (500 ppb), and excellent selectivity. Moreover, the performance of the sensor in practical applications was evaluated by detecting the gas released during *Larimichthys crocea* (~500 g) spoilage process at 25 and 4°C. Herein, 10 ppm TMA was set as the onset of the fish spoilage. Combining the results of sensor response and GC–MS analysis, it was concluded that when *L. crocea* was kept at 4°C, it took 7 days to the status of initial corruption, while the fish only took 3 days at 25°C. Additionally, the ambient

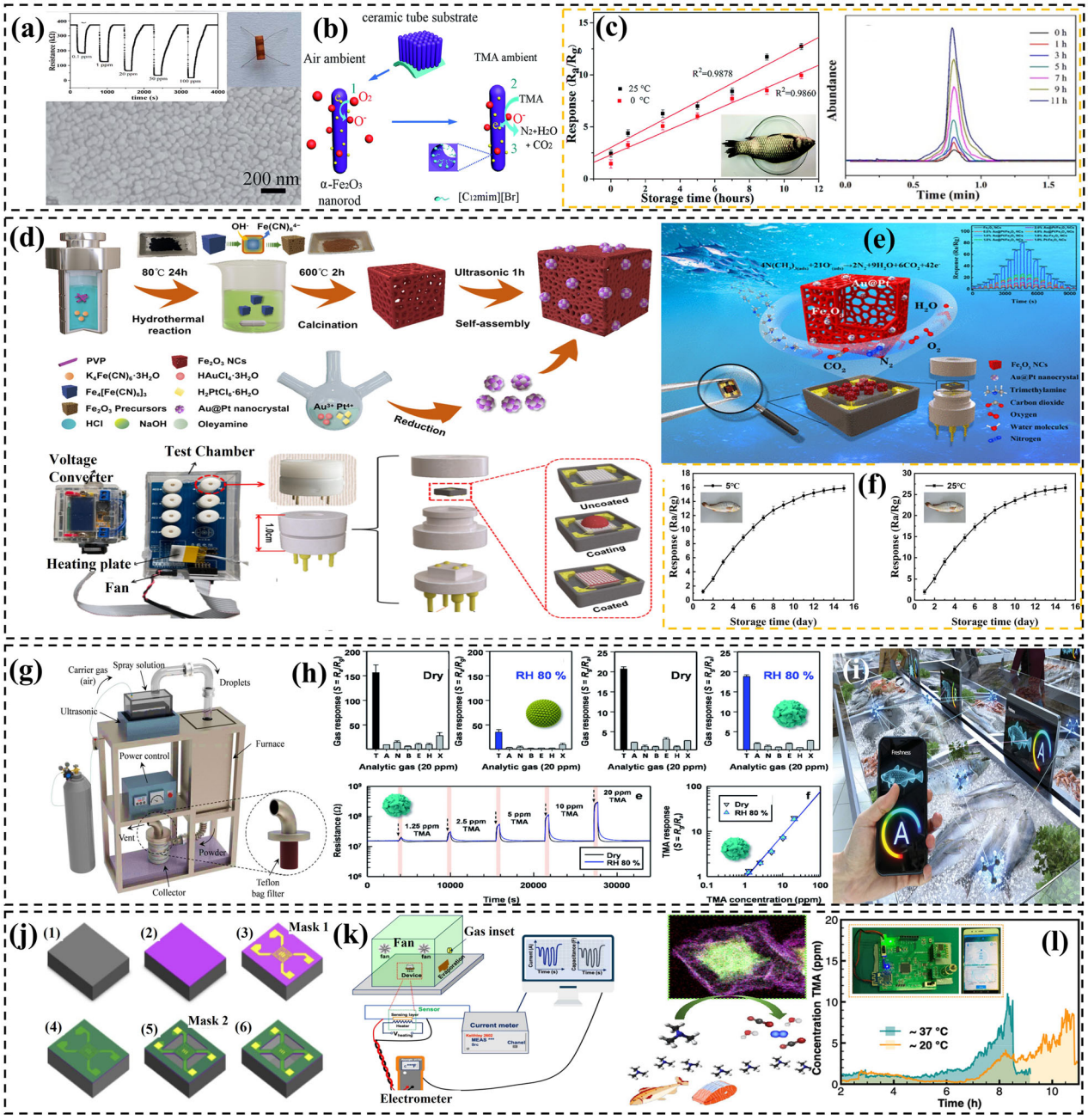

FIGURE 2 α-Fe_2O_3 mesoporous nanorod array TMA sensor (Wang et al., 2017): (a) microstructure of α-Fe_2O_3 mesoporous nanorods, photo of the sensor, and dynamic response to TMA; (b) schematic diagram of the gas-sensing mechanism of α-Fe_2O_3 sensor to TMA; and (c) the response of α-Fe_2O_3 sensor to the crucian carp freshness at 0 and 250°C, and the gas chromatogram of crucian carp within 0–11 h. Au@Pt/α-Fe_2O_3 TMA sensor (Shen et al., 2021): (d) preparation process and sensor test system; (e) schematic diagram of the TMA sensing mechanism; and (f) sensor detection results of large yellow croaker freshness. $Pr_{0.2}Ce_{0.8}W_9O_{33}$ anti-humidity interference TMA sensor (Kim et al., 2021): (g) schematic diagram of the preparation of the sensor; (h) response characteristics of the sensor to TMA under different humidity conditions; and (i) application of the sensor in the field of fish freshness detection. Co_3O_4@ZnO nanocage TMA sensor (Yan et al., 2021): (j) schematic diagram of the fabrication process of the sensor; (k) schematic diagram of the sensing test system and its gas-sensing mechanism to TMA; and (l) real-time results of the sensor detecting fish freshness

humidity may significantly impact the performance stability and freshness evaluation accuracy of WO_3-based gas sensors, especially for devices with lower operating temperatures. To address such problems, Kim et al. prepared $Ce_4W_9O_{33}$ and Pr–$Ce_4W_9O_{33}$ powders with porous structures by ultrasonic spray pyrolysis (Figure 2g) and low-temperature annealing (Kim et al., 2021). The sensing material and terpineol-based ink were then milled at a mass ratio of 2:3 to obtain a viscous paste, which was screen-printed onto alumina with two Au electrodes to fabricate the sensor. This work reports the $Pr_{0.2}Ce_{0.8}W_9O_{33}$ gas sensor and its TMA-sensing properties against humidity interference. As shown in Figure 2h, when the test environment changed from 0% to 80% relative humidity (RH), the resistance and gas response values of the pure WO_3 sensor decreased significantly, and the selectivity decreased. But the $Pr_{0.2}Ce_{0.8}W_9O_{33}$ semiconductor exhibited almost similar gas-sensing properties, including high response ($R_g/R_a = 22$ at 20 ppm) and high selectivity, stability, and linear correlation. The anti-humidity sensing properties could be ascribed to the unique interaction among the Ce^{3+}, Pr^{3+}, and $(WO_4)^{2-}$, electron sensitization, and enhanced surface reactivity, which enabled the sensor to be resistant to ambient moisture by eliminating surface hydroxyl groups. In addition, the surface acidity of $Pr_{0.2}Ce_{0.8}W_9O_{33}$ also helps to enhance the gas-sensing properties. This work is demonstrated to have utility for fish freshness detection (Figure 2i) and provides a new general strategy for designing humidity-resistance gas sensors.

MOSR TMA sensors have become a research hotspot because of their high compatibility with integrated circuits. However, resistive-type TMA sensors still present challenges in seafood spoilage monitoring, such as cross-response to interference gases with similar molecular structure or adsorption activity (e.g., DMA and NH_3), limited linear response range, and baseline signal drift. In response to the above limitations, porous core–shell composites have been extensively studied as the advanced gas-sensing material. They provide interfacial heterojunctions (either electronically or chemically sensitized), and the permeability of the shell and internal voids will offer more surface reaction sites to facilitate the reaction between the adsorbed oxygen ions and target gas, thereby enhancing the gas-sensing performance. Yan et al. designed Co_3O_4@ZnO porous hollow nanocages-based TMA sensor and verified its practical application capability (Yan et al., 2021). First, hollow and porous Co_3O_4@ZnO nanocages were prepared using metal–organic frameworks (MOFs) ZIF-67@ZIF-8 template. Subsequently, the microsensor equipped with two Pt interdigitated electrodes and a serpentine heating element was fabricated using microelectromechanical machining process (Figure 2j). The resistive response of this sensor to TMA was evaluated using a self-made sensing test system and its gas-sensing mechanism was elucidated (Figure 2k). The sensor exhibited high response, high immunity to humidity interference, high baseline stability, and rapid response/recovery to TMA (3/2 s at 33 ppm), while almost nonexistent to other gas cross-response. In order to further verify the practicality of the Co_3O_4@ZnO sensor in seafood spoilage detection, the sensor was integrated into a portable device with Bluetooth function for real-time detection of hairtail freshness changes at different storage temperatures (Figure 2l). Before testing, approximately 200 g samples and sensor equipment were placed at both ends of a storage tank (8 L). The results showed that the response values were very low at the beginning, and the response values and the TMA concentration increased significantly over time, revealing that the hairtail began to deteriorate. Finally, when the jar was opened to introduce fresh air, the reading of the sensor dropped to the original baseline. According to reported works, 4 ppm TMA was identified as the spoilage threshold for a 200-g hairtail sample. The fresh time of hairtail at around 37°C (8.5 h) was shorter than at around 20°C (10.8 h), indicating that it is more susceptible to spoilage at higher temperatures. The resistive sensing device demonstrated a proof-of-concept for hairtail spoilage detection, showing promising application potential.

In addition, more metal oxides have also shown application potential in TMA detection, such as binary metal oxides (ZnO, Co_3O_4, In_2O_3, V_2O_5, WO_3) and ternary metal oxides ($NiFe_2O_4$, $ZnFe_2O_4$, $CoMoO_4$, $NiGa_2O_4$). Table 2 summarizes the preparation techniques and performance parameters of various MOSR TMA gas sensors. MOSR TMA sensors show good gas-sensing properties under different test conditions and good application prospects.

3.2 | Triethylamine

TEA, released by microbial degradation during fish spoilage, is also one of the markers worth noting. Therefore, the realization of sensitive, accurate, and real-time detection of TEA gas is beneficial to ensuring food safety and human health. However, the concentration of released TEA is low. For example, the concentration of TEA released from rotten crucian carp (~200 g) at ambient temperature for 7 days is not higher than 4 ppm (Li, Chu, et al., 2019). Hence, lower gas concentrations pose new challenges to the gas sensor. This section will summarize the development of MOSR TEA gas sensor for fish freshness detection in the past 5 years.

With its high thermal and chemical stability, ZnO is widely used as an n-type semiconductor in the gas-sensing field. However, for TEA, the corresponding performance of

TABLE 2 MOSR gas sensors for trimethylamine detection

Materials	Methods	Morphology	Temp.	Conc.	Response	τ_{res}/τ_{rec}	LOD (ppm)	Selectivity	Stability (≥)	References
MoO_3	Hydrothermal	Nanobelts	240°C	5 ppm	36.4[a]	~15/50 s	1	Good	–	Yang et al., 2016
$CoMoO_4/MoO_3$	Hydrothermal and dipping	Nanobelts	220°C	10 ppm	25.2[a]	~10 s/–	5	Good	30 days	Li, Song, et al., 2018
$MoO_3/Bi_2Mo_3O_{12}$	Solvothermal	Hollow microspheres	170°C	10 ppm	7.2[a]	~20/100 s	0.1	Good	90 days	Zhang et al., 2019
α-MoO_3	Solvothermal	Nanosheets	133°C	10 ppm	51.47[a]	~15/300 s	0.02	Good	90 days	Shen et al., 2019
$MoO_3/MoSe_2$	Hydrothermal	Flowers-rods	RT	1 ppm	3.9[a]	~12/19 s	0.02	Good	30 days	Zhou et al., 2021
α-Fe_2O_3	Hydrothermal	Nanorods	217°C	50 ppm	14.9[a]	~1/70 s	0.1	Good	100 days	Wang et al., 2017
α-Fe_2O_3	Solvothermal	Nanospheres	250°C	20 ppm	7.1[a]	~100/200 s	1	Good	60 days	Liu, Fu, et al., 2020
α-Fe_2O_3	Solvothermal	Snowflakes	260°C	100 ppm	10.9[a]	~0.1/1.5 s	5	Poor	–	Yang et al., 2017
Au@Pt/α-Fe_2O_3	Wet chemical	Hollow cubes	150°C	100 ppm	32.0[a]	~5/74 s	1	Good	30 days	Shen et al., 2021
WO_3	Spray pyrolysis	Hollow spheres	450°C	5 ppm	56.9[a]	~1.5/486 s	0.05	Good	–	Cho et al., 2013
Au–WO_3	Hard template synthesis	Mesoporous	268°C	100 ppm	42.56[a]	~1/323 s	5	Good	17 days	Wang, Zhang, et al., 2021
$PdO/WO_{2.72}$	Solvothermal	Urchin-like microspheres	260°C	40 ppm	496.6[a]	~16/57 s	–	Good	30 days	Shang et al., 2020
$Au/PdO/WO_{2.72}$	Photo-deposition		240°C	40 ppm	802.5[a]	~4/44 s	–	Good	30 days	
ZnO	Wet chemical and calcined	Nanorods arrays	400°C	5 ppm	3.5[a]	~9/5 s	–	Fine	–	Meng et al., 2019
Pd–ZnO			300°C	5 ppm	5.5[a]	~7/7 s	1	Good	50 days	
Au–ZnO	Wet chemical	Porous nanosheets	260°C	30 ppm	65.8[a]	~3.3/64 s	0.1	Fine	21 days	Meng et al., 2017
Au/ZnO	Self-templated synthesis	Nanospheres	250°C	10 ppm	52.6[a]	12/127 s	0.4	Fine	30 days	Chen et al., 2022
Co_3O_4/ZnO	Wet chemical and calcined	Nanocages	190°C	10 ppm	149.1[a]	~2/11.8 s	0.013	Good	–	Li, Li, et al., 2020
In_2O_3	Hydrothermal	Nanocubes	160°C	10 ppm	57.0[a]	~4/11 s	–	Good	15 days	Zhang et al., 2018
In_2O_3	Electrospinning	Nanofibers	80°C	10 ppm	5.5[a]	~6/10 s	1	–	–	Li, Liu, et al., 2020
Mo–Co_3O_4	Spray pyrolysis	York-shell spheres	250°C	5 ppm	71.4[b]	~25/350 s	0.5	Good	–	Kim et al., 2019
Co_3O_4@ZnO	Wet chemical and calcined	Hollow cages	250°C	33 ppm	41.0[a]	~3/2 s	0.33	Good	30 days	Yan et al., 2021
V_2O_5	Hydrothermal	Flower-like spheres	200°C	5 ppm	2.17[a]	~13/13 s	1	Good	60 days	Meng et al., 2020
Graphene–$NiGa_2O_4$	Hydrothermal	Nanoparticles	20°C	5 ppm	11.2[a]	~7/112 s	0.01	Good	7 days	Chu et al., 2020
Cr_2O_3–SnO_2	Template synthesis	Inverse opals	275°C	5 ppm	301.3[a]	~73/40 s	0.0056	Good	21 days	Park et al., 2020
TiO_2–$NiFe_2O_4$	Hydrothermal	Nanoparticles	307°C	10 ppm	11.2[b]	~50/45 s	0.1	Good	30 days	Wang, Zhang, et al., 2022
Pr–$Ce_4W_9O_{33}$	Spray pyrolysis	Hollow spheres	350°C	10 ppm	8.2[b]	~150/345 s	1.25	Good	–	Kim et al., 2021

Note: –, not mentioned.
Abbreviation: RT, room temperature (25 ± 5°C).
[a] $S = R_a/R_g$.
[b] $S = R_g/R_a$.

ZnO, even at a higher working temperature, is still insufficient and cannot meet the actual detection requirements. Designing special nanostructures or using noble metal elements to modify the surface of pure ZnO semiconductors can effectively enhance the TEA-sensing properties. Shen et al. prepared hierarchically porous ZnO microspheres assembled by nanosheets by a simple precipitation method. They grew Ag nanoparticles on the surface to prepare Ag–ZnO composite material (Shen et al., 2018). The Ag–ZnO sensor had a response value of 6043 to 100 ppm TEA at 183.5°C, which was 15 times that of the pristine ZnO sensor. The response/recovery time of Ag–ZnO was 1/60 s (100 ppm TEA), with a detection limit of 0.5 ppm, as well as fine TEA selectivity and stability, benefiting from the porous hierarchical nanostructure and the sensitization effect of Ag nanoparticles. In addition, the bonding type between Zn^{2+} and O^{2-} in ZnO is mainly ionic bonding, so it is suitable for doping with main group metals or transition metal ions (Cu, Fe, Mn, Ni, Co). The s and p electrons of ZnO will interact with the d electrons of transition metal ions to affect its electronic properties and gas-sensing properties. From the perspective of practical application, Fan et al. synthesized Co-doped ZnO precursor powders at near room temperature and obtained Co–ZnO composites through high-temperature calcination treatment, which exhibited a two-dimensional porous nanodisc structure (Fan et al., 2021). The crystal defects generated by Co ion doping and its catalytic effect enabled the Co–ZnO nanocomposites to obtain significantly improved response ($R_a/R_g = 28$ at 10 ppm TEA) and lowered detection limit of 200 ppb. More importantly, the Co–ZnO-based sensor was insensitive to ambient humidity and had fine operational stability.

Introducing a second phase is also an effective strategy to enhance the gas-sensing properties of MOSR sensors. Ma et al. utilized MOFs to derive In_2O_3/ZnO composites (Figure 3a) with flower-like structures assembled from nanorods (providing a large specific surface area), heterojunctions, and a unique multielectron surface interfacial transport process (improving electron transfer efficiency) (Ma et al., 2021). The In_2O_3/ZnO sensor exhibited ideal TEA-sensing properties, including high response (75.5 at 10 ppm TEA), long-term operational stability, and fast response/recovery speed. In addition, the TEA released by a whole crucian carp at different storage times was detected to elucidate its working principle and verify the practicality of the In_2O_3/ZnO sensor (Figure 3b). The actual concentrations of TEA gas were estimated to be 15.49, 24.17, 36.19, 75.77, and 158.15 ppm for fish within 1–5 days. This work provides a simple approach for rapid nondestructive testing of fish freshness.

Tungsten trioxide (WO_3), as a kind of typical n-type semiconductor, has a narrow bandgap and excellent charge transfer ability, which will help to improve the signal-to-noise ratio of the sensor, thus being beneficial to its practical application. Chen et al. reported a TEA sensor based on single-crystal WO_3 nanosheets and studied the effect of the thickness of the gas-sensing layer on the sensor performance (Chen et al., 2018). The 5-nm WO_3 nanosheet sensor exhibited the good linear response to 10–200 ppm TEA at 25°C with the response values of 1.2–8.9 (R_a/R_g). Gu et al. reported a TEA sensor based on Pt (II)-modified ordered macroporous WO_3 (SA-Pt/WO_3) (Figure 3c) (Gu et al., 2019). Compared with Pt particles or agglomerates, atomically dispersed Pt could increase the amounts of active regions and reduce the activation energy required for the reaction, thereby enabling the high-performance detection of TEA (Figure 3d). The SA-Pt/WO_3 exhibited good sensitivity (28.4 ppm^{-1}) to TEA and a low detection limit (0.18 ppb), and the response value for 10 ppm TEA could reach 270. Furthermore, the high electron-donating TEA molecules will be selectively absorbed on the uniform isolated Pt (Pt_{iso}) atom sites due to the strong interaction and efficient charge transfer between Pt_{iso} atom sites and WO_3, leading to a higher response to TEA than to other gases, that is, high selectivity. The SA-Pt/WO_3 gas sensor was also used to detect the fish freshness. First, the crucian carp fillets were put into a sealed bottle (1.5 L). It was then stored at 25°C, and the gas (100 ml) at different storage times was taken as a sample to detect and analyze the spoilage degree of the fish. As shown in Figure 3e, the decay rate of the fish (200 g) increased after being stored for 6 h, and the sensor response value rapidly increased to 65 after being stored for 12 h, indicating that the crucian carp was in the decay stage or even completely decomposed. In addition, the practicality of the sensor was also verified by detecting different masses of crucian carp (100, 200, 400 g) under the same storage time (12 h).

In practical applications, the changes in ambient humidity will have a greater impact on the performance stability (sensitivity and response/recovery speed) and freshness assessment accuracy of TEA gas sensors, especially for devices with lower operating temperatures. To solve such problems, Zhu et al. prepared hydrophobic inorganic CeO_2/SnO_2 heterostructure films gas sensors, demonstrating excellent gas-sensing properties to TEA with high response, wide detection range (0.04–500 ppm), low detection limit (0.04 ppm), and long-term stability, while possessing promising anti-humidity sensing ability (Zhu et al., 2022). Xiong et al. synthesized two-dimensional ultrathin ZnO/Co_3O_4 heterostructure nanomeshes by in situ growth technology (Xiong et al., 2021). Compared to the pure Co_3O_4 and ZnO sensors, the gas sensor based on ZnO/Co_3O_4 nanomesh achieved a lower operating temperature (from 300 to 100°C) and exhibited higher response values ($R_a/R_g = 3.2$ at 5 ppm TEA) and faster

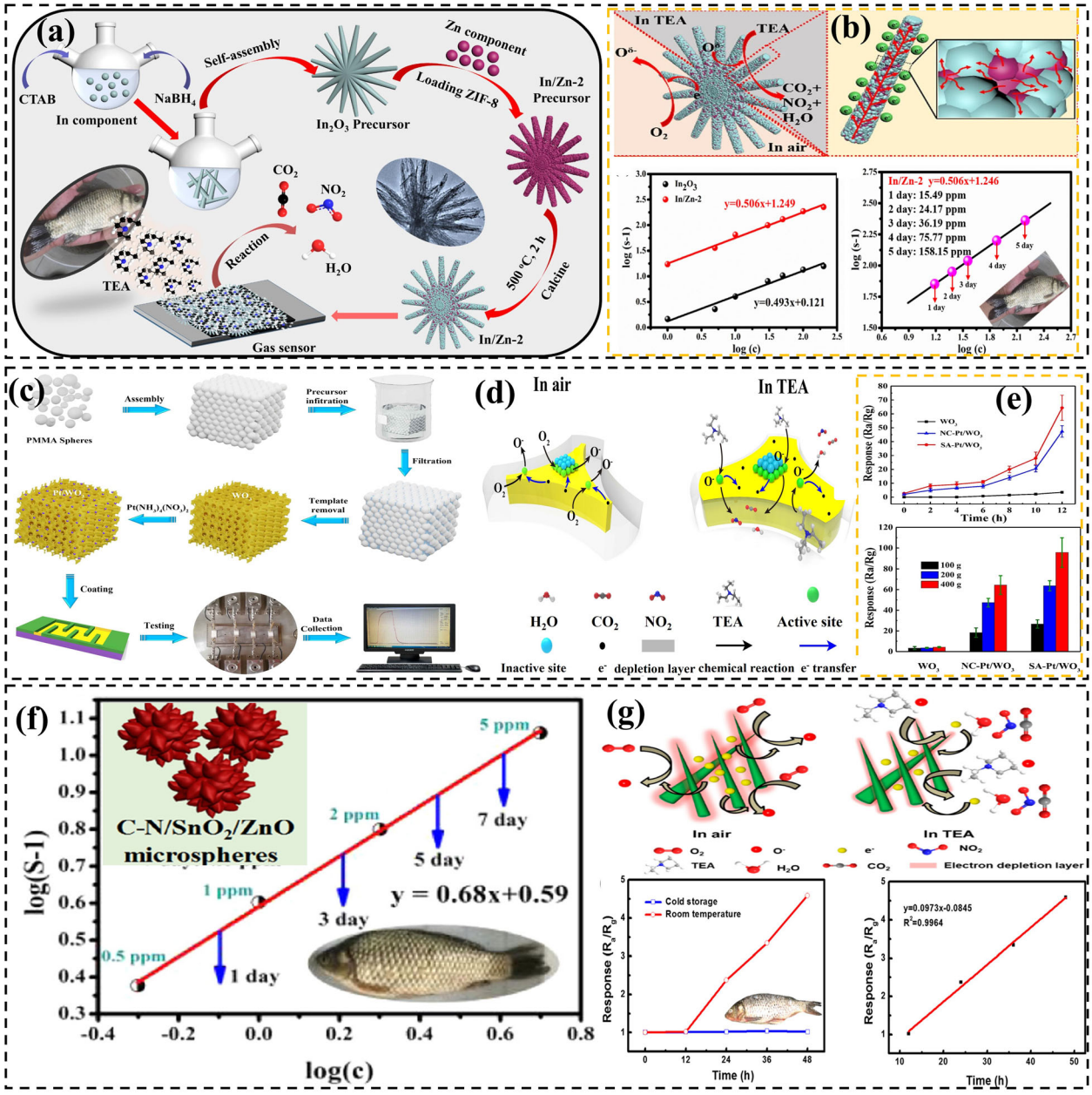

FIGURE 3 Flower-like In_2O_3/ZnO composite TEA sensor (Ma et al., 2021): (a) synthesis route of In_2O_3/ZnO gas-sensing material and application of sensor; (b) schematic diagram of TEA gas-sensing mechanism of the sensor and the results of the sensor's detection of fish freshness at different storage times. Pt (II)–WO_3 macroporous array TEA sensor (Gu et al., 2019): (c) schematic diagram of the synthesis route and gas-sensing material and sensor testing system; (d) the test results of Pt (II)–WO_3 sensor to different weights of crucian carp. (f) The detection results of C–N/SnO_2/ZnO/Au composite TEA sensor on the crucian carp freshness at different storage times (Li, Chu, et al., 2019). (g) Schematic diagram of the gas-sensing mechanism of the needle-like WO_3 nanorod TEA sensor and the application of the sensor in the field of fish freshness detection (Hu et al., 2020)

response/recovery (30/55 s at 5 ppm TEA) at 100°C. With mesoporous structure, abundant surface oxygen defects, and p–n heterostructure, the ZnO/Co_3O_4 sensor still had a rapid detection under a wide RH range (25%–85% RH). The response value only fluctuated slightly, showing a strong practical application potential. Furthermore, under extreme conditions such as high RH, ensuring efficient detection, excellent selectivity, and fast response/recovery speed for lower concentrations of TEA (ppb level) remains challenging for TEA gas sensing. Wang et al. designed and fabricated the WO_3–$W_{18}O_{49}$ composite with a hierarchical macroporous structure. The WO_3–$W_{18}O_{49}$ surface was functionalized with glucose and PdO particles to obtain multiple heterostructures and chemical/electronic

sensitization effects (Wang, Han, et al., 2022). The sensor exhibited good TEA gas-sensing performance at 325°C, including excellent selectivity and an extremely low detection limit (R_a/R_g = 1.5 at 50 ppb TEA). In addition, the multicomponent semiconductor gas sensor maintains high response ($R_a/R_g \approx 20$ at 50 ppm TEA) and shorter response/recovery time (1/2 s at 50 ppm TEA).

In addition, a gas sensor with linear response to TEA gas will enable nondestructive determination and prediction of fish freshness. Li et al. prepared C–N/SnO_2/ZnO–Au composite gas-sensitive layer with uniform size via a single spinneret electrospinning-calcination treatment in situ reduction method (Li, Chu, et al., 2019). The composite gas sensor exhibited ultrahigh response and excellent selectivity to 0.5–100 ppm TEA under the synergistic enhancement of multiple components. It could complete the response and recovery to 50 ppm TEA within 30 s. The practical application potential of the sensor was verified by detecting the volatile odor of crucian carp (around 200 g) stored at 80°C within different storage periods (0.25, 1, 3, 5, and 7 days). The specific method is to extract 5 ml volatiles from the storage bottle as the target gas after being stored for various times and use the sensor to detect and record the response characteristics at different stages. As shown in Figure 3f, the gas responses obtained after 0.25, 1, 3, 5, and 7 days of storage were approximately 2.0, 4.3, 6.4, 8.9, and 11.0, respectively. According to the acquired two-dimensional correlation of sensor response-gas concentration, the concentrations of volatile gases at different stages were calculated to be 0.13, 0.8, 1.6, 2.8, and 4.0 ppm, respectively. The good linear relationship makes the C–N/SnO_2/ZnO–Au sensor promising for rapid fish freshness detection. Hu et al. fabricated the needle-like WO_3 nanorods-based TEA sensor (Hu et al., 2020). The as-fabricated sensor was then placed at 400°C for 3 days to enhance long-term stability. The sensor test results exhibited that the response of the sensor to 1 ppm TEA could reach 6 (R_a/R_g), the response to 50 ppm TEA was about 120, and it exhibited excellent selectivity. The detection of the odor of grass carp (200 g) verified the practical feasibility of the sensor. As shown in Figure 3g, grass carp were sealed and stored at 25 and 4°C, respectively. After being stored for 0, 12, 24, 36, and 48 h, 10 ml volatiles were extracted from it and injected into an 18-L airtight box. Refrigeration can effectively delay decay, but the sensor response value increased from 1.02 to 4.59 within 12–48 h at room temperature, and the decay rate was faster. Therefore, the study recommended that dead fish should be eaten within 12 h or stored refrigerated below 4°C.

In addition, more types of metal oxides have also shown application potential in the field of TEA chemiresistive gas sensors, such as single metal oxides (Co_3O_4, In_2O_3, TiO_2) and double metal oxides ($NiCo_2O_4$, $ZnFe_2O_4$). Table 3 summarizes the fabrication techniques and performance parameters of various MOSR TEA gas sensors for fish freshness detection.

3.3 | Ammonia

Fish in the process of spoilage is difficult to detect visually compared to completely spoiled fish. Therefore, it is very important and meaningful to conduct a timely and accurate evaluation of fish quality. It is worth noting that after the death of the fish, the spoilage bacteria in the fish will cause the decomposition of urea and amino acids of fish to produce NH_3. Therefore, for high-protein foods such as fish, the volatilized NH_3 can be used as a fish freshness indicator. This section summarizes the development of this type of gas sensor in the past 5 years.

To meet practical application standards, gas sensors with high selectivity and low detection limit have become a research focus in food freshness detection, including fish. Wu et al. prepared nanosheet-assembled $CuFe_2O_4$ hollow microspheres by a facile solvothermal synthesis method (Wu, Xu, et al., 2021). Thanks to the special spinel crystal structure, hollow structure, and large specific surface area, the $CuFe_2O_4$ sensor exhibited good gas-sensing performance for ppm-level NH_3 at 100°C and 49% RH, including good selectivity, low detection limit (1 ppm), and cycling stability. Chou et al. reported a WO_3 thin-film NH_3 sensor fabricated by radio frequency sputtering (Chou et al., 2019). The WO_3 film with a thickness of 10 nm exhibited good gas-sensing performance, including a high response value (13.7 at 1000 ppm NH_3, 250°C), low detection limit (10 ppb), effective detection concentration range (0.01–1000 ppm), and excellent selectivity. In addition, the sensor has the advantages of simple structure and easy fabrication, which is expected to be used for practical applications in low-concentration NH_3 detection. Tonezzer et al. used single tin oxide nanowires as gas-sensing material to detect 0.1–5 ppm NH_3 at different working temperatures (200–360°C). The fabricated resistive SnO_2 sensor was used to nondestructively test the freshness of trout (*Oncorhynchus mykiss*), mackerel fish (*Scomber scombrus*), and Salmo trutta marmoratus (Tonezzer, 2021a, 2021b; Tonezzer et al., 2021). The microbiological analysis was also carried out to verify the good correlation of the sensor response to the TVCs. TVC was measured on plate count agar and agar media (Oxoid CM0463 and 0055, Hampshire, UK) using the diffusion plate technique. The experimental results showed that the sensor response at different temperatures had a good correlation with the TVC, indicating that it was a better indirect method for measuring the bacterial count. In addition, samples stored at different temperatures were classified

TABLE 3 MOSR gas sensors for triethylamine (TEA) detection

Materials	Methods	Morphology	Temp.	Conc.	Response	τ_{res}/τ_{rec}	LOD (ppm)	Selectivity	Stability (≥)	References
Co–ZnO	Precipitation and calcination	Nanodiscs	280°C	10 ppm	27.5[a]	~8/16 s	0.2	Good	60 days	Fan et al., 2021
Ag–ZnO	Hydrothermal and calcination	Microspheres	183.5°C	100 ppm	6043[a]	~1/60 s	0.5	Fine	30 days	Shen et al., 2018
In_2O_3/ZnO	Solvothermal	Flower-like	120°C	100 ppm	188.0[a]	~58/215 s	0.32	Good	30 days	Ma et al., 2021
C–N/SnO_2/ZnO/Au	Electrospinning and calcination	Microspheres	80°C	50 ppm	55.0[a]	~15/6 s	0.5	Good	30 days	Li, Chu, et al., 2019
$ZnFe_2O_4$–ZnO	Solvothermal	Coral-like	240°C	50 ppm	21.3[a]	~0.9/23 s	0.5	Fine	–	Yang et al., 2020
Co_3O_4	Sacrificial template	Hollow microtubes	180°C	200 ppm	3.5[b]	~13/81 s	1	Good	35 days	Hu et al., 2022
ZnO/Co_3O_4	Hydrothermal	Nanomeshes	100°C	5 ppm	3.2[a]	~30/55 s	–	Good	35 days	Xiong et al., 2021
Au–α-Fe_2O_3/rGO	Hydrothermal	Nanospheres	250°C	100 ppm	43.6[a]	~5/7 s	–	Good	30 days	Liu, Song, et al., 2020
α-Fe_2O_3/NiO	Hydrothermal	Hierarchical microspheres	140°C	10 ppm	10.8[a]	~18/59 s	0.8	Good	30 days	Bai et al., 2020
Sn–NiO	Electrospinning and calcination	Hollow nanofibers	180°C	100 ppm	16.6[b]	~39/11 s	0.5	Good	31 days	Yang, Han, et al., 2021
SnO_2	Hydrothermal	Nanorods	120°C	50 ppm	64.0[a]	~6/465 s	–	Good	50 days	Xu et al., 2021
Au–SnO_2/ZnO	Hydrothermal-pulsed laser deposition direct current (DC) sputtering	Core–shell nanorods	40°C	10 ppm	12.4[a]	~1.2/75 s	–	Fine	31 days	Ju et al., 2015
In_2O_3	Chemical conversion	Microtubes	300°C	0.1 ppm	1.9[a]	~103/117 s	0.1	Good	14 days	Yang et al., 2018
CuO/TiO_2	Water bath-etching	Nanoparticles	160°C	5 ppm	12.7[a]	~45/202 s	0.5	Fine	30 days	Wang et al., 2019
WO_3–$W_{18}O_{49}$	Hydrothermal	Urchin-like	325°C	100 ppm	35.7[a]	~1/2 s	0.05	Good	17 days	Wang, Han, et al., 2022
$NiCo_2O_4$	Hydrothermal	Nanoplate	220°C	10 ppm	2.58[b]	~33/42 s	0.5	Good	30 days	Zhao et al., 2020

Note: –, not mentioned.

[a] $S = R_a/R_g$.

[b] $S = R_g/R_a$.

(100%) using a PCA method with log (TVC) errors below 5%, and a machine learning algorithm was then used to determine the spoilage stage of the fish and estimate their TVC. Therefore, the electronic nose can not only classify their freshness, but also quantitatively evaluate the concentration of microorganisms. Due to its tiny size (0.1 mm), economy, ease of operation, and detection speed, the sensor will likely be a practical tool in noninvasive freshness detection.

Although these sensors show good sensing characteristics, the operating temperature is still high, which will cause the problem of grain growth, which will lead to selectivity drift and destabilize the operation of the sensor. Moreover, the selectivity also needs to be further improved. Therefore, high-precision gas sensors for detecting NH_3 at 25 ± 5°C have gradually been reported in recent years. To obtain the high-performance sensing properties of TiO_2 nanomaterials to NH_3, Wu et al. used a trace amount of rare earth element cerium to dope TiO_2 nanocrystals. The synergistic enhancement strategy based on small-sized nanostructures, high specific surface area, induced high-energy facet growth, and modified surface states was developed (Figure 4a) (Wu, Debliquy, et al., 2022). The sensor exhibited excellent NH_3-sensing properties at room temperature, such as high response (23.99 at 20 ppm), low detection limit (140 ppb), excellent selectivity, and operation stability. In addition, fish spoilage detection was also studied using homemade measuring equipment, and the schematic diagram of its working principle is shown in Figure 4a. First, the thawed fillets (Pangasius, 25 g) were stored in a 0.6-L airtight bottle at 25°C, subsequently, using a small air pump to inject spoilage gas into the testing box, and the gas flow during test procedure was 500 ml/min. When assessing fish freshness in this work, 5 ppm NH_3 was used as the indicator for the onset of fish spoilage (this can be changed depending on the part of the fish or storage conditions). The test results (Figure 4b) showed that the NH_3 concentration was lower than 5 ppm for 6 h, showing that the fish maintained acceptable quality. Within 12–24 h, the released NH_3 exceeded 6 ppm, and the fish was in the spoilage stage, confirming the practical potential of the Ce–TiO_2 gas sensor.

Furthermore, the challenges of humidity interference, unsatisfactory device integration, and automation level of room-temperature NH_3 sensors also limit their practical application in the field and real-time food quality monitoring. To this end, Zhang et al. designed a composite sensing material based on (001) TiO_2 and two-dimensional transition metal carbides ($Ti_3C_2T_x$) (Figure 4c) (Zhang, Yu, et al., 2022). (001) TiO_2 crystal facet with high surface activity can provide efficient photogenerated electrons under UV light illumination, and $Ti_3C_2T_x$ can keep holes by the Schottky junction generated with TiO_2, which can effectively avoid the re-combination of electrons and holes, thus enhancing the NH_3-sensing properties. The results showed that the sensor had a response value of 40.6 to NH_3 (30 ppm), a detection limit of 156 ppt, excellent selectivity, and strong resistance to humidity interference (test range: 10%–82% RH) under the excitation of UV light. The fabricated sensor was used to monitor the NH_3 released from 100 g fish during storage at 25°C and 25% RH to verify its practical potential. In this work, NH_3 concentrations thresholds were set as 1 and 5 ppm to indicate the onset and complete spoilage of fish. As shown in Figure 4d, the NH_3 concentration in the fish was lower than 1 ppm within 13 h, revealing the fish still maintained fine freshness. However, within 18–36 h, the NH_3 concentration quickly reached above 10 ppm, indicating the decay rate increased rapidly under the microorganisms' action. To further improve its portability and automation, the research group designed a smart alarm device including NFC and a microcontroller system (Figure 4e). When (001) $TiO_2/Ti_3C_2T_x$ sensor detects the dead fish, the released NH_3 gas will generate a resistance signal, which will be transmitted to the microcontroller at the same time, and the signal will be detected by an NFC-enabled smartphone. When the smartphone detects the sensor's signal, the liquid crystal display will display the current meat freshness status and light up. The device was used to detect the current state of fish during 36-h storage. A green light indicated the fish was fresh and safe to eat within 13 h of storage at 30°C. When the (001) $TiO_2/Ti_3C_2T_x$-based sensor detected the fish within 13–24 h, a yellow light will illuminate. The red light will work if the detected gas concentration exceeded 5 ppm, indicating the fish had started to deteriorate. Therefore, this sensing technology will have excellent prospects in food quality monitoring.

Possessing a certain degree of flexibility (such as bending fatigue resistance) will meet the needs of applications that have special requirements for device flexibility, thereby broadening the application of gas sensors in the field of fish freshness detection. Therefore, it is very meaningful to develop flexible gas sensors. Li et al. designed a flexible, humidity-independent room-temperature NH_3 sensor. The 100-nm CeO_2–CuBr gas sensor was fabricated by depositing porous nanoscale CuBr particles on flexible PI substrates by thermal evaporation, followed by deposition of a CeO_2 capping layer by electron beam evaporation (Figure 4f) (Li, Lee, et al., 2018). At room temperature, the sensor showed a high response, fine selectivity, rapid response and recovery, and an extremely low detection limit (20 ppb NH_3). The CeO_2 layer acts as a barrier to moisture interaction with CuBr (Figure 4g). Due to the presence of the CeO_2 overlay, the sensor resistance and gas response remained constant regardless of humidity changed from dry (RH 0%) to RH 80%.

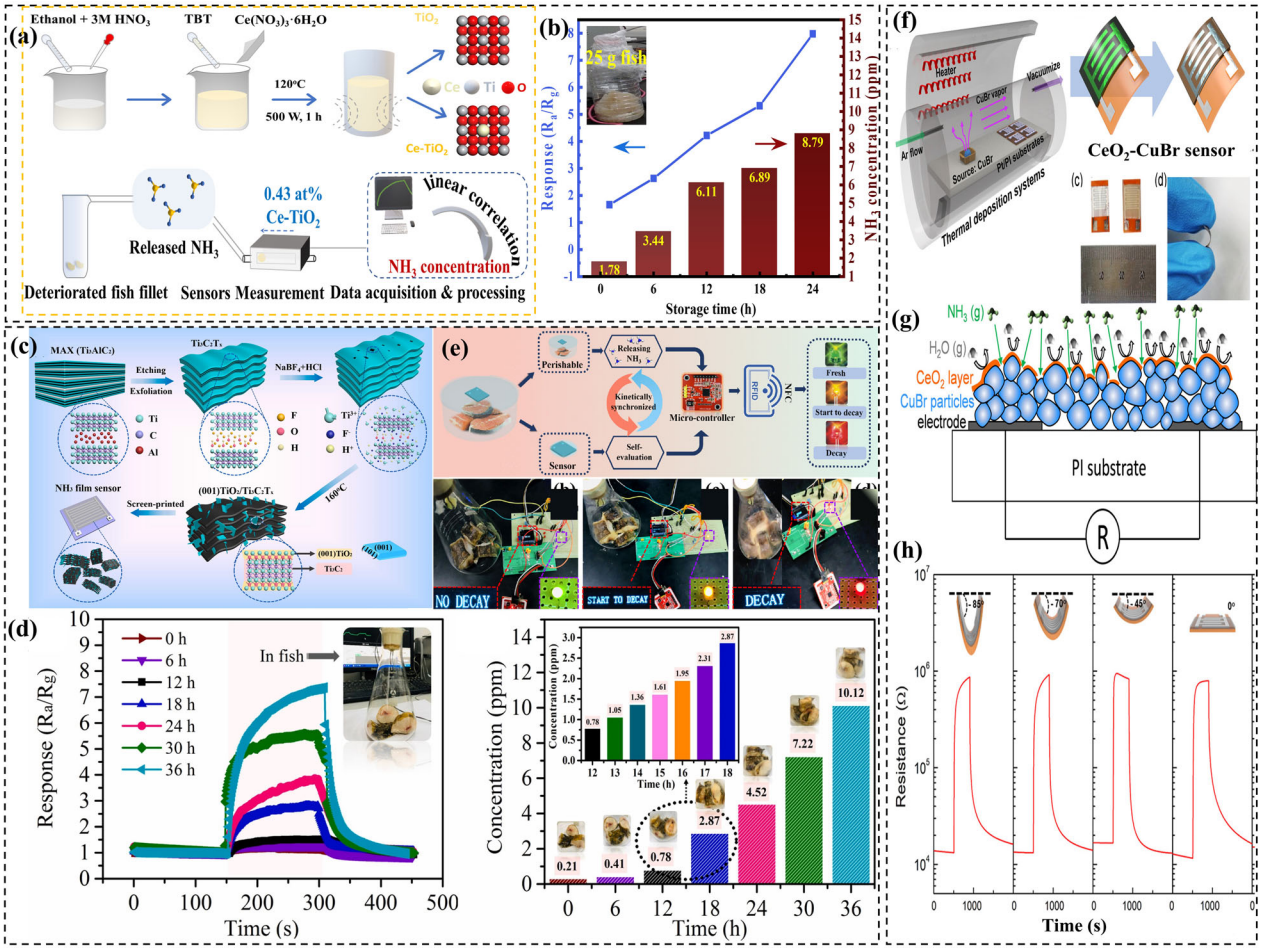

FIGURE 4 Room-temperature NH_3 sensor based on Ce–TiO_2 nanocrystals (Wu, Debliquy, et al., 2022): (a) schematic diagram of the synthesis route of Ce–TiO_2 gas-sensing material and the detection principle of fish freshness; (b) the results of sensor detection of the freshness of pangasius at different storage times. Room-temperature NH_3 sensor based on (001) $TiO_2/Ti_3C_2T_x$ composites (Zhang, Yu, et al., 2022): (c) schematic diagram of the synthesis route of $TiO_2/Ti_3C_2T_x$ gas-sensing materials and the sensor fabrication; (d) a graph of the response to different concentrations of ammonia during the detection of fresh fish rotting; (e) a block diagram of an integrated circuit alarm system and status indicators for fish that are "not rotting," "starting to rotting," and "rotting." CeO_2–CuBr room-temperature NH_3 sensor (Li, Lee, et al., 2018): (f) schematic diagram of preparation process of CeO_2–CuBr sensor; (g) NH_3 gas-sensing mechanism and anti-humidity interference mechanism of CeO_2–CuBr sensor; (h) flexible performance of the sensor

Furthermore, thanks to the flexibility of the PI substrate and the well-deposited porous sensing film, the sensor exhibited high stability under various bending conditions (−85° to +85°) (Figure 4h). The gas response value remained almost unchanged after 2000 bends at 45°. The small changes upon bending at large angles are attributed to the reduced connectivity between CuBr particles. The room-temperature flexible NH_3 sensor will provide a new technology for rapid nondestructive detection of fish freshness under different environmental conditions.

Table 4 summarizes the preparation technology and performance parameters of MOSR gas sensors targeting NH_3 (one of the signs of fish spoilage) in the past 5 years. The reported resistive semiconductor NH_3 sensors showed good gas-sensing characteristics and device integration properties under different test conditions, which will show a broad application prospect in practice.

3.4 | Other target gases

In addition to the above three signature gases, fish will release a small number of other signature gases in the process of spoilage, such as MMA, DMA, H_2S, DMS, DMDS, and so forth. This section will summarize the development overview of MOSR sensors for the above target gases in the past 5 years.

TABLE 4 MOSR gas sensors for NH_3 detection

Materials	Methods	Morphology	Temp.	Conc.	Response	τ_{res}/τ_{rec}	LOD (ppm)	Selectivity	Stability (≥)	References
WO_3	RF sputtering	10-nm films	250°C	100 ppm	5.1[a]	~108/160 s	0.01	Good	–	Chou et al., 2019
SnO_2	Chemical vapor deposition	Nanowires	300°C	5 ppm	3.0[a]	~9/9 s	0.1	–	–	Tonezzer et al., 2021
$CuFe_2O_4$	Solvothermal	Hollow microspheres	100°C	10 ppm	4.0[a]	~32/190 s	1	Fine	–	Wu, Xu, et al., 2021
TiO_2	Microwave-assisted solvothermal	Nanocrystals	RT	20 ppm	6.3[a]	~83/228 s	0.29	Fine	–	Wu, Debliquy, et al., 2022
Ce–TiO_2					23.99[a]	~55/192 s	0.14	Good	7 days	
Ag–TiO_2	Etching and calcination	Microspheres	RT	25 ppm	22.3[a]	~36/168 s	5	Good	15 days	Wen et al., 2022
TiO_2/MXene	Etching and hydrothermal	Lamellar	RT, UV (365 nm)	30 ppm	40.6[a]	~13/81 s	0.005	Good	150 days	Zhang, Yu, et al., 2022
CeO_2–CuBr	hydrothermal	Thin films	RT	5 ppm	68.0[b]	~200/1055 s	0.02	Good	–	Li, Lee, et al., 2018

Note: –, not mentioned.
Abbreviation: RT, room temperature (25 ± 5°C).
[a] $S = R_a/R_g$.
[b] $S = R_g/R_a$.

3.4.1 | MMA and DMA

MMA and DMA are widely used in a variety of industrial applications. They are flammable and explosive, have a strong irritating odor, and pose a significant threat to human health. For example, long-term exposure to higher than 10 ppm DMA can cause respiratory and eye damage. In addition, such gases are also present in seafood. In addition to volatilizing TMA, the concentration of methylamines, such as MMA and DMA, will also increase during the decomposition and decay of fish. Therefore, the concentration of methylamines is related to the assessment of seafood quality and methylamines are recommended as biomarker gases for evaluating fish freshness. Currently, the quantitative monitoring of volatile methylamines in seafood can be achieved using gas chromatography, capillary electrophoresis, and so forth. However, several limitations remain, such as complicated equipment and long time for sample preparation. Therefore, it is very important to develop gas sensors for real-time monitoring methylamines (MMA, DMA). This section summarizes the development of this type of gas sensor in the past 5 years.

Bruce et al. used a simple wet chemical method to directly grow flower-like ZnO on the interdigital electrode to prepare the MMA sensor, but the response value of the pure ZnO to 400 ppm MMA at 250°C was only 1.82 (R_a/R_g). It is difficult to meet the actual detection requirements (Bruce et al., 2022). In order to obtain higher response, the research group modified the ZnO surface with noble metal Pd catalyst particles, which effectively induced a larger variation in the electron depletion layer and resistance, thereby enhancing the sensing performance. The Pd–ZnO sensor showed a high response (200) toward 400 ppm, and the effective detection range was 25–400 ppm. Although the sensor showed high response, the selectivity had not been evaluated, and the operating temperature is high, which easily leads to the secondary growth of ZnO grains and reduces the operational stability of the sensor. Galstyan et al. successfully synthesized a TiO_2 tubular structure by anodization method. The experiments showed that the tubular TiO_2 had high selectivity for DMA. However, it had low response. When detecting 10 ppm DMA at 300°C, the sensor had almost no response (Galstyan et al., 2020). The niobium (Nb) element was introduced into the titania tubular structure to enhance the gas adsorption capacity to enhance its gas-sensing properties further. The response of the as-prepared Nb-doped TiO_2 (Nb–TiO_2) to 10 ppm DMA was improved from 1.14 to 4.6, and the interference response of other volatile organic compounds (VOCs) and NH_3 to the sensor was negligible, which significantly improved the selectivity. However, the sensor also had a high working temperature, which

will limit its wide application in the field of fish freshness detection.

Therefore, the development of room-temperature methylamine sensors has gradually become one of the new research hotpots. Srinivasan et al. rapidly prepared a series of MoO_3 nanomaterials by microwave hydrothermal synthesis. In order to avoid the formation of agglomerated particles and affect the gas-sensing performance, MoO_3 nanorods with uniform distribution, twinning dislocation, and controlled aspect ratio were obtained by calcination (Srinivasan & Rayappan, 2021). The existence of twinning dislocations will increase its surface activation energy, thereby promoting the adsorption of oxygen on the surface of MoO_3 and its ability to adsorb and react with target gas molecules at lower working temperatures. The sensor showed a response value of about 2.1 (R_a/R_g) toward 1 ppm DMA at 30°C and a response/recovery time of 23/12 s. In the range of 32%–83% RH, the response fluctuation to DMA was only 9%, and the selectivity and cycling stability are good. The detection limit of the sensor is much lower than the threshold (10 ppm) of the volatile gas of fish spoilage, so the sensor can be used to detect fish freshness rapidly. Ganesan et al. used DC reactive magnetron sputtering technology to deposit a highly uniformly distributed TiO_2 film on a glass substrate, and obtained the film with the best structure and performance by adjusting the substrate temperature (Ganesan et al., 2020). The TiO_2 thin-film gas sensor had a response value (R_a/R_g) of 82 at room temperature (~27°C) to 4 ppm DMA and a response/recovery time of 210/150 s. In addition, MOSs are generally responsive to DMA and other amines, such as TMA and NH_3, but TiO_2 films showed high selectivity to DMA. At the same time, the sensor's low detection limit (0.4 ppm) also meets the criteria for practical applications. In order to realize the high-performance room-temperature sensing properties of TiO_2 for low-concentration (ppb) DMA, Yang et al. prepared a PANI/TiO_2 composite gas-sensing material using the conductive organic polymer polyaniline (PANI) as the reinforcing phase (Yang, Zhang, et al., 2021). The PANI/TiO_2 sensor exhibited a response of 2.8 toward 10 ppm DMA at 25°C and high selectivity (no response to 30 ppm TMA and NH_3). The sensor also showed a good linear response range (R^2 = .995 at 0.05–30 ppm), and the detection limit was low as 0.05 ppm. This work will provide a new strategy for room-temperature detection of DMA.

The metal oxide gas sensing materials summarized above are all n-type semiconductors. P-type semiconductors have also been reported in fish spoilage gas (such as DMA) sensors due to their physical nature, such as wide band gap, high dielectric constant, and high stability. Sovizi and Mirzakhani (2020) synthesized the rare earth element oxide La_2O_3 by the reverse micelle method, and La_2O_3 exhibited two-dimensional nanoplates assembled from nanoparticles. After testing, the La_2O_3 gas sensor had a response (R_g/R_a) of 3.1 to 10 ppm DMA at room temperature and could complete the full response/recovery behavior within 80 s, especially the recovery speed was extremely fast (<10 s), which had a good selectivity and operating stability (the response value was stable at about 9 within 480 h). The excellent gas sensing properties give the p-type La_2O_3 gas sensor potential for fish freshness detection. However, in the past 5 years, the research on p-type semiconductors gas sensors is limited, and there is still a large development space and prospects, such as the improvement of sensitivity, the decrease of signal-to-noise ratio, and the improvement of humidity resistance.

Table 5 summarizes the preparation technology and performance parameters of MOSR gas sensors targeting MMA and DMA in the past 5 years. The reported resistive gas sensors showed fine gas sensing properties at different test conditions, which can be the promised candidates for practical application.

3.4.2 | H_2S, DMS, and DMDS

In the case of microbial spoilage, 10 ml protein will generate at least about 100 μg of sulfide gas (H_2S, DMS, DMDS, etc.) within a few hours, so fish freshness can be indirectly monitored by sulfide gas sensors. Based on the fish stock size and temperature parameters, the sulfide gas detection limit of the sensor system must be below 100 ppb. MOSR gas sensors are currently the most commercialized devices, which possess high response, low cost, and easy operation. Therefore, it is significant to develop MOSR gas sensors for real-time monitoring of sulfides (H_2S, DMS, and DMDS). This section will summarize the development of this type of gas sensor in the past 5 years.

H_2S

The detection of trace target gases with high selectivity and sensitivity is a major challenge in practical applications. To overcome this critical problem, a series of MOSR gas sensors with extremely low detection limits have been developed and reported in recent years. Zhang et al. reported the flower-like α-$Bi_2Mo_3O_{12}$ nanomaterials-based H_2S sensor. Benefiting from the good chemical reaction ability of $Bi_2Mo_3O_{12}$, the sensor achieved efficient and rapid detection of H_2S (3/22 s at 100 ppm) at 133°C, reducing the detection limit to 1 ppb. The sensor also maintained a stable response in the humidity range of 10%–95% RH (Zhang, Zheng, et al., 2022). Yang et al. fabricated a network-like nano-walled NiO gas sensor with a large pore size and high crystallinity through in situ growth

TABLE 5 MOSR gas sensors for methylamine detection

Materials	Methods	Morphology	Temp.	Conc.	Response	τ_{res}/τ_{rec}	LOD (ppm)	Selectivity	Stability (≥)	References
Pd–ZnO	Wet chemical	Nanoflowers	250°C	25 ppm (MMA)	1.43[a]	~210/180 s	–	–	–	Bruce et al., 2022
TiO_2	Anodic synthesis	Nanotubes	300°C	10 ppm (DMA)	1.1[a]	~1050/810 s	–	Good	–	Galstyan et al., 2020
Nb–TiO_2					4.6[a]	~900/450 s	5	Good	–	
TiO_2	Sol–gel and hydrothermal	Nanorods	217°C	30 ppm (DMA)	2.6[a]	–	–	–	–	Yang, Zhang, et al., 2021
PANI/TiO_2	Gas-phase diffusion	Forest-like	RT	10 ppm (DMA)	2.8[a]	~42/12 s	0.05	Good	30 days	
β-Bi_2O_3	Chemical spray pyrolysis	nanoparticles	RT	10 ppm (DMA)	12.1[a]	~15/75 s	0.5	Fine	180 days	Pandeeswari et al., 2022
MoO_3	Microwave-assisted hydrothermal	nanorods	RT	20 ppm (MMA)	39.0[a]	~23/12 s	–	Fine	30 days	Srinivasan & Rayappan, 2021
TiO_2	Reactive DC magnetron sputtering	nanoparticles	RT	4 ppm (DMA)	82.0[a]	~210/150 s	0.4	Good	30 days	Ganesan et al., 2020
La_2O_3	Reverse micelle	nanoparticles	RT	10 ppm (DMA)	3.1[b]	~72/8 s	3	Good	20 days	Sovizi & Mirzakhani, 2020

Note: –, not mentioned.

Abbreviation: RT, room temperature (25 ± 5°C).

[a] $S = R_a/R_g$.

[b] $S = R_g/R_a$.

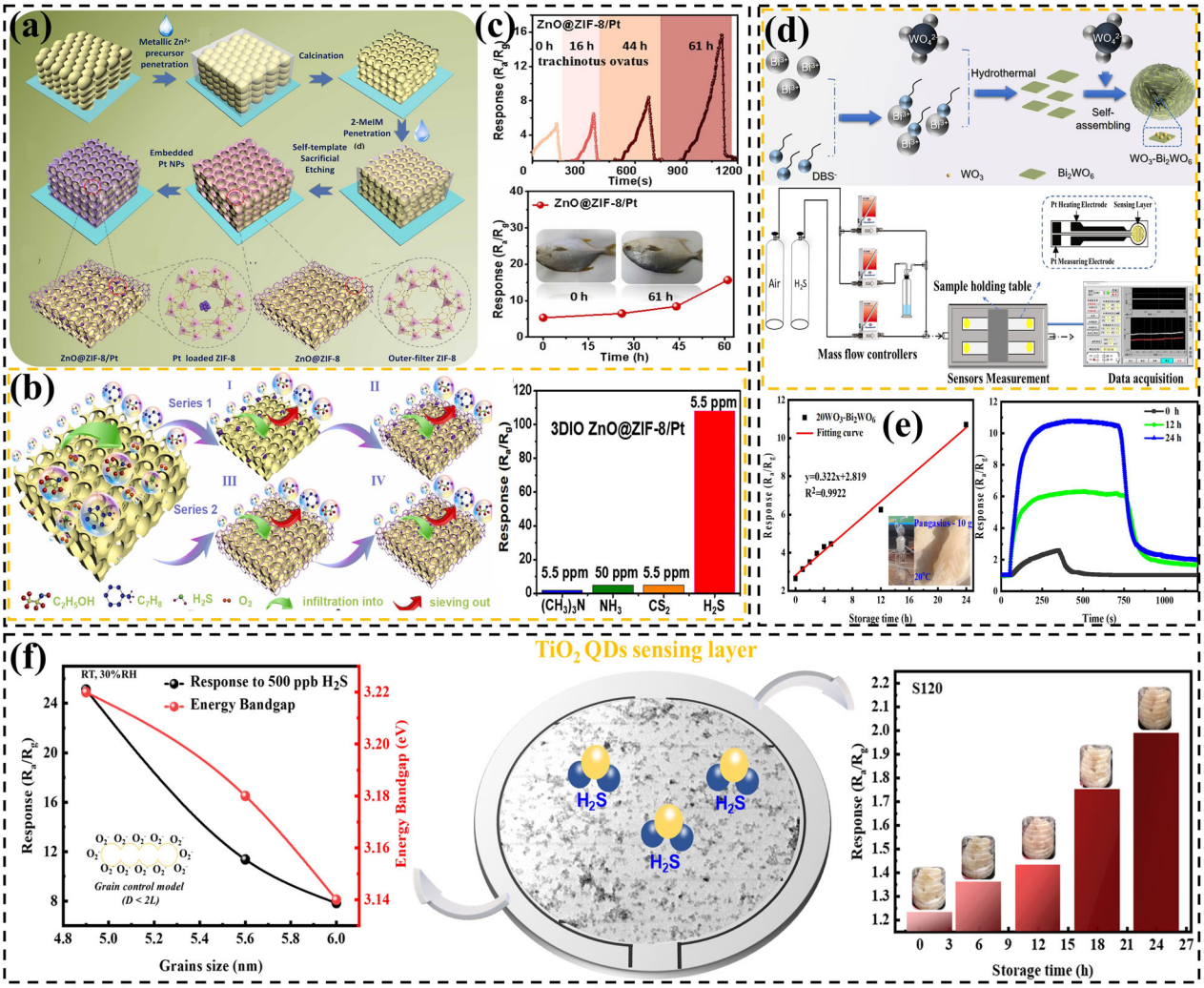

FIGURE 5 Inverse opal structure of ZnO@ZIF-8/Pt H_2S sensor (Zhou et al., 2022): (a) schematic diagram of the preparation process of ZnO@ZIF-8/Pt gas-sensing material; (b) the selectivity enhancement mechanism and actual selectivity test of ZnO@ZIF-8/Pt; (c) detection results of the fish freshness stored for different storage times. Room-temperature WO_3–Bi_2WO_6 composite H_2S sensor (Zhang, Wu, et al., 2022): (d) synthesis route of WO_3–Bi_2WO_6 gas-sensing material and schematical diagram of sensor test system; (e) the detection results to the odor of pangasius stored at 20°C. (f) TiO_2 quantum dots H_2S sensor working at room temperature (Wu, Zhang, et al., 2022): the sensing properties of the sensor to 500 ppb H_2S, the H_2S gas-sensing mechanism, and the sensor's fish spoilage detection performance

technique. The NiO gas sensor exhibited an obvious and reversible response toward 0.01–100 ppm H_2S at 50°C, the response toward 100 ppm H_2S reached 137.3, and the detection limit was 10 ppb. Additionally, the sensor showed good selectivity, humidity resistance, and long-term stability (Yang et al., 2019). Zhou et al. designed a multicomponent composite gas-sensing material (ZnO@ZIF-8/Pt) based on macroporous ZnO, ZIF-8 layered molecular sieves, and Pt nanoparticles with inverse opal structure (Figure 5a) (Zhou et al., 2022). Notably, the macroporous structure and the introduction of Pt particles effectively enhanced surface chemisorption capacity and the transfer efficiency of gas molecules and free electrons. Moreover, the ZIF-8 layer reduced the interference response of VOCs with larger kinetic diameters (Figure 5b). The gas-sensing test results showed the ZnO@ZIF-8/Pt obtained high response (118 at 5.5 ppm H_2S), low detection limit (40 ppb), and excellent selectivity. To verify its practicality, the ZnO@ZIF-8/Pt sensor was used to detect the changes in H_2S concentration released by crucian carp under room-temperature storage conditions. As shown in Figure 5c, the response value gradually increased along with the longer spoilage time. After 61 h, the sensor response toward crucian carp was as high as 16, corresponding to an H_2S concentration of about 2.2 ppm, while the color of crucian carp darkened after 61 h. Furthermore, the gas chromatograph was used to measure the gas released after crucian carp spoilage for 61 h, mainly H_2S, TMA, NH_3, and carbon disulfide (CS_2). In order to verify whether there is interference from other gases, TMA, NH_3, and CS_2 were tested separately,

and it was found that the sensor only showed a very low response for other gases (including 50 ppm NH_3), revealing the responses in the above test results were mainly from H_2S (Figure 5c). It indicated that this work provides more reliable and accurate information for fish freshness assessment.

Lowering the operating temperature of the sensor can simplify the sensor device structure and improve the operation stability (Liu et al., 2022). Therefore, room-temperature gas sensors for rapid fish freshness detection have become a research hotspot in recent years. Zhang et al. developed a novel bismuth tungstate-based composite gas sensor for efficiently detecting NH_3 at room temperature. Tungsten oxide–bismuth tungstate microflower (WO_3–Bi_2WO_6) gas sensor was prepared using a facile hydrothermal synthesis method and drop coating technique (Zhang, Wu, et al., 2022). Figure 5d is a schematic diagram of the synthetic route and the gas-sensing test system. The sensor exhibited a good response to 2–50 ppb H_2S at room temperature ($R_a/R_g = 4.4$ at 50 ppb), and the detection limit was 2 ppb. And it still performed an obvious response to ppb-level H_2S in the humidity range of 30%–70% RH. The excellent sensing performance was attributed to the synergistic strategy of the catalytic effect of WO_3 particles, the hierarchical nanostructure of Bi_2WO_6, and the n–n heterostructures. To verify the practicability of the sensor, the pangasius was used as the detection object, and the WO_3–Bi_2WO_6 gas sensor was used to detect fish freshness at room temperature (20°C) (Figure 5e). As the storage time became longer, the response value increased from 2.6 to 10.7, and showed good linearity, proving its practicality. Wu et al. rapidly prepared size-controlled titania quantum dots (TiO_2 QDs) by microwave-assisted synthesis route for detecting ppb-level H_2S (Wu, Zhang, et al., 2022). The TiO_2 QDs gas sensor exhibited good sensing performance for 100–500 ppb H_2S at room temperature, including a high response (25.12 at 500 ppb H_2S), fast response (34 s at 500 ppb), low detection limit level, and good selectivity. The synergistic effect of ultrasmall-size nanostructures and modified surface characteristics improved the charge transfer efficiency, thereby effectively enhancing the room-temperature gas sensing properties. In addition, the application of TiO_2 QDs in detecting volatile substances in fish (25 g, Pangasius) stored at room temperature was also studied. In Figure 5f, the response value of the TiO_2 QDs increased from 1.24 to 2.01 in 24 h. In addition, the optical photos of the fish also showed that the fish had darkened during storage, indicating that the fish had begun to spoil. These results confirm the application potential of TiO_2 QDs gas sensors for low concentration H_2S detection.

DMS and DMDS

Volatile sulfur compounds, including DMDS and DMS, are also a component of spoilage volatile gases in some fish, such as cod (Duflos et al., 2006b). Therefore, the sensors with volatile sulfur compound as the target gas have also been reported recently. Zhang et al. prepared perovskite lanthanum ferrite ($LaFeO_3$) and neodymium ferrite ($NdFeO_3$) nanoparticles by sol–gel method, and fabricated gas sensors by solution drop coating method. The p-type $LaFeO_3$ gas sensor showed a response value of 16.5 (R_g/R_a) to 10 ppm DMS, and the $NdFeO_3$ gas sensor showed a response value of 17.2 (R_g/R_a) to 10 ppm DMDS. The cross-response experiments also proved that other gases (including CO, NO_2, and ethanol) did not interfere with either response. In addition, these sensors showed good stability to the changes in ambient humidity (11–95% RH) (Zhang et al., 2021). To overcome the insufficient improvement of the performance of MOSR DMDS gas sensors from single metal modification, Liu et al. prepared AuPd/SnO_2 hollow sphere gas sensor materials using the in situ reduction method. Combining the characterization and gas-sensing test results, they found that the loading of AuPd effectively tuned the electronic structure and gas reaction path of the sensing layer, greatly improving the response (16.3 at 5 ppm) and the selectivity to DMDS. The DMDS-sensing enhancement mechanism of AuPd/SnO_2 material was elucidated by first-principles calculations (Density functional theroy, DFT) and in situ characterization techniques. In addition, the introduction of AuPd alloy improved the electronic structure of SnO_2 and enhanced the electron affinity of AuPd/SnO_2 surface for DMDS, thereby obtaining ultrahigh selectivity to DMDS (Liu et al., 2021). The excellent gas-sensing performance will give it application potential in the field of rapid fish freshness detection.

Table 6 summarizes the synthesis methods and performance parameters of MOSR gas sensors targeting H_2S, DMS, and DMDS in the past 5 years. These reported gas sensors showed good gas sensing performance under different test conditions, including the low detection limit and rapid response speed.

In conclusion, the reported MOSR gas sensors showed good sensing properties to single target gas for fish freshness detection. Compared to the standard methods (GC, GC–MS, HPLC, and ion mobility spectrometry) for determining the various biomarker gases, MOSR gas sensors show significant advantages, such as rapid detection, high sensitivity, low energy consumption, real-time monitoring, easy operation, and nondestructive detection. However, there also exist several disadvantages, such as environmental factors (temperature and humidity), that may affect

TABLE 6 MOSR gas sensors for volatile sulfide compounds detection

Materials	Methods	Morphology	Temp.	Conc.	Response	τ_{res}/τ_{rec}	LOD (ppb)	Selectivity	Stability (≥)	References
CuO	Hydrothermal	Nanosheets	325°C	400 ppb (H_2S)	1.7[b]	~210/180 s	3	Fine	7 days	Miao et al., 2020
Pd–CuO	Co-precipitate	Nanoflowers	80°C	10 ppm (H_2S)	63.8[b]	~15 s/–	100	Good	42 days	Hu et al., 2017
α-$Bi_2Mo_3O_{12}$	Solvothermal	Flower-like	133°C	1 ppm (H_2S)	1.9[a]	~9/10 s	1	Good	60 days	Zhang, Zheng, et al., 2022
NiO	Liquid deposition	Meshed nanowalls	50°C	1 ppm (H_2S)	6.0[b]	~300/1200 s	10	Good	60 days	Yang et al., 2019
ZnO@ZIF-8/Pt	Self-template synthesis	Inverse opal	310°C	5.5 ppm (H_2S)	118.0[a]	~60/280 s	40	Good	80 days	Zhou et al., 2022
WO_3–Bi_2WO_6	Hydrothermal	Microflowers	RT	50 ppb (H_2S)	4.4[a]	~52/119 s	2	Good	7 days	Zhang, Wu, et al., 2022
TiO_2	Microwave-solvothermal	Quantum dots	RT	500 ppb (H_2S)	25.1[a]	~34/470 s	100	Good	7 days	Wu, Zhang, et al., 2022
$LaFeO_3$	Citrate sol–gel method	Nanoparticles	210°C	10 ppm (DMS)	16.5[b]	–	–	Fine	15 days	Zhang et al., 2021
$NdFeO_3$				10 ppm (DMDS)	17.2[b]	–	–			
AuPd/SnO_2	Solvothermal & reduction	Hollow spheres	135°C	5 ppm (DMDS)	19.5[a]	~49/20 s	100	Good	16 days	Liu et al., 2021

Note: –, not mentioned.
Abbreviation: RT, room temperature (25 ± 5°C).
[a] $S = R_a/R_g$.
[b] $S = R_g/R_a$.

detection accuracy and cross-sensitivity to interference gases, leading to failure determination of the gases or volatile organic compounds. Therefore, the sensing technology for detecting multiple odor indicators is developed, which will be discussed in the next part.

4 | GAS SENSOR ARRAY, ELECTRONIC NOSE TECHNOLOGY, AND THEIR APPLICATION

Sensory analysis is a standard and commonly accepted method for assessing fish freshness. But the method suffers from extremely low automation, high subjectivity, poor reproducibility, and limitations related to fatigue or adaptation. In addition, sensory analysis, as a nonquantitative method, requires multiple professional evaluators for its high-precision results, which may also lead to high costs. In the absence of rapid and cheap alternatives to sensory analysis, the detection techniques based on gas sensor arrays offer an interesting choice for fish freshness assessment, which is low cost and rapid compared to other methods. Seafood, including fish, has multiple odor indicators for freshness evaluation, so using a combination of indicators to assess freshness will significantly improve the reliability of the results (Chang et al., 2017; Tang & Yu, 2020). Therefore, the gas sensor arrays or electronic nose technology with various released gases as detection targets has become an emerging method to determine freshness (Zambotti et al., 2019, 2020). This section will summarize recent advances in gas sensors (arrays), electronic nose technology, and their applications for multiple odors.

4.1 | Gas sensors (arrays) for multiple odors and their applications

Srinivasan et al. prepared different ZnO nanostructures (nanoaggregates and nanospheres) by hydrothermal synthesis and sol–gel method to detect the markers of fish freshness (NH_3, C_3H_9N, and C_2H_6S) (Srinivasan & Rayappan, 2020). The dual-sensing properties of ZnO nanoaggregates toward NH_3 and C_3H_9N had fast response/recovery and good operation stability, with the highest response values (R_a/R_g) of 1207 and 758, respectively. The detection limit of ZnO nanoaggregates for NH_3 and C_3H_9N is lower than 5 ppm. Additionally, the ZnO nanosphere exhibited good selectivity to C_2H_6S at room temperature with a detection limit below 5 ppm. Moreover, the responses of the two nanostructures under different RH conditions showed fine stability, verifying the practicality of these sensors in fish quality analysis. Senapati et al. designed and constructed the Ag–SnO_2–

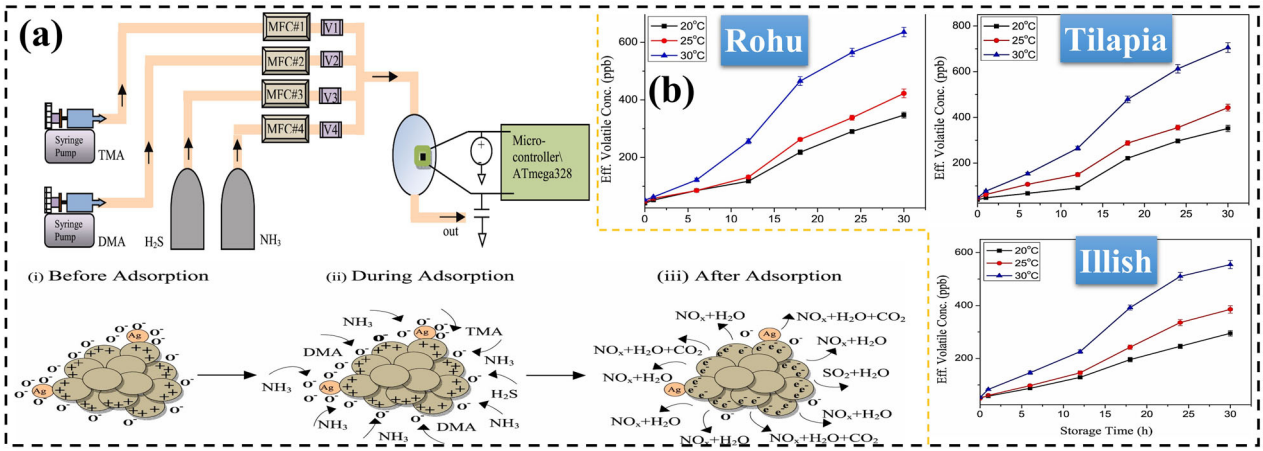

FIGURE 6 Ag–SnO_2–SiO_2-Si sensor array (Senapati & Sahu, 2020): (a) experimental setup for calibrating the Ag–SnO_2–SiO_2–Si sensor with known concentrations of volatile gases (NH_3, H_2S, DMA, and TMA) and the array's response to the target gas detection mechanism; (b) volatile concentrations detected by sensor arrays versus storage time in Rohu, Tilapia, and Illish at 20, 25, and 30°C

SiO_2–Si gas sensor array for real-time detection of fish freshness (Figure 6a) (Senapati & Sahu, 2020). Based on the gas-sensing mechanism shown in Figure 6a, the sensor exhibited good sensing characteristics to the volatile gases (NH_3, TMA, DMA, and H_2S), including high response and repeatability. In addition, the sensor was used to detect the released gases from Rohu, Tilapia, and Illish fish stored at 20, 25, and 30°C, respectively (Figure 6b), then combining with the results of total volatile basic nitrogen and TVCs, a rapid assessment of the freshness of the three types of fish was achieved. Notably, the effective volatile concentration at 20°C is close to that obtained at 25°C, but due to the increased microbial activities at higher temperatures the rate of increase of volatile concentration for the temperature at 30°C is much higher. Using this technique, the safe edible periods of Rohu, Tilapia, and Illish fish stored at 25°C were 17, 16, and 14 h, respectively. The rapid detection technique reported in this work has commercial utility in fish freshness detection at room temperature.

4.2 | Electronic nose

Inspired by the mammalian olfactory system, a bionic technology (electronic nose) based on sensor arrays has emerged (Grassi et al., 2022). The electronic nose simulates biological function to recognize some simple or complex smell (Güney & Atasoy, 2015). Figure 7a,b summarizes the main components of electronic nose technology and their corresponding biological functions and various analysis schemes for sensor array signals. The electronic nose is composed of three parts: sensor array, odor signal acquisition and preprocessing, and pattern recognition. When a certain smell comes into contact with the sensor array, each sensor will convert the chemical signal of the reaction process into a physical electrical signal. After pattern recognition and analysis, the sensor array will finally recognize the overall information of the volatile components in the smell just like the sense of smell (El Barbri et al., 2007). Compared with traditional chemical instrument analysis methods (such as GC–MS, HPLC, etc.), the electronic nose omits a series of complex pretreatment processes, such as organic solvent extraction, while it also has a short detection time, fast speed, and wide application range. Compared with the separated gas sensors, the electronic nose uses multiple target gases to improve the reliability of determining freshness, while electronic nose can process the cross-response results using a specific algorithm. Electronic nose can identify the smell of various kinds of food and agricultural products, especially some gases that are inconvenient for people to directly contact, such as VOCs with a strong irritating smell and even poisonous gases (Jia et al., 2019; Li, Geng, et al., 2020; Wang et al., 2018). Therefore, this technology shows a good application prospect for monitoring, discriminating, and analyzing gases in different fields, especially in the food industry.

In recent years, electronic noses have been widely reported as a nondestructive method for food quality inspection, such as classifying stored grains, identifying water quality, detecting the freshness of fish and fruits, and detecting bacterial growth in meat and vegetables. Among them, the application of the electronic nose in the detection of fish and its byproducts' freshness has attracted much attention. Leghrib et al. designed and built a portable gas detection system for fish freshness monitoring based on five commercial semiconductor resistive gas sensors

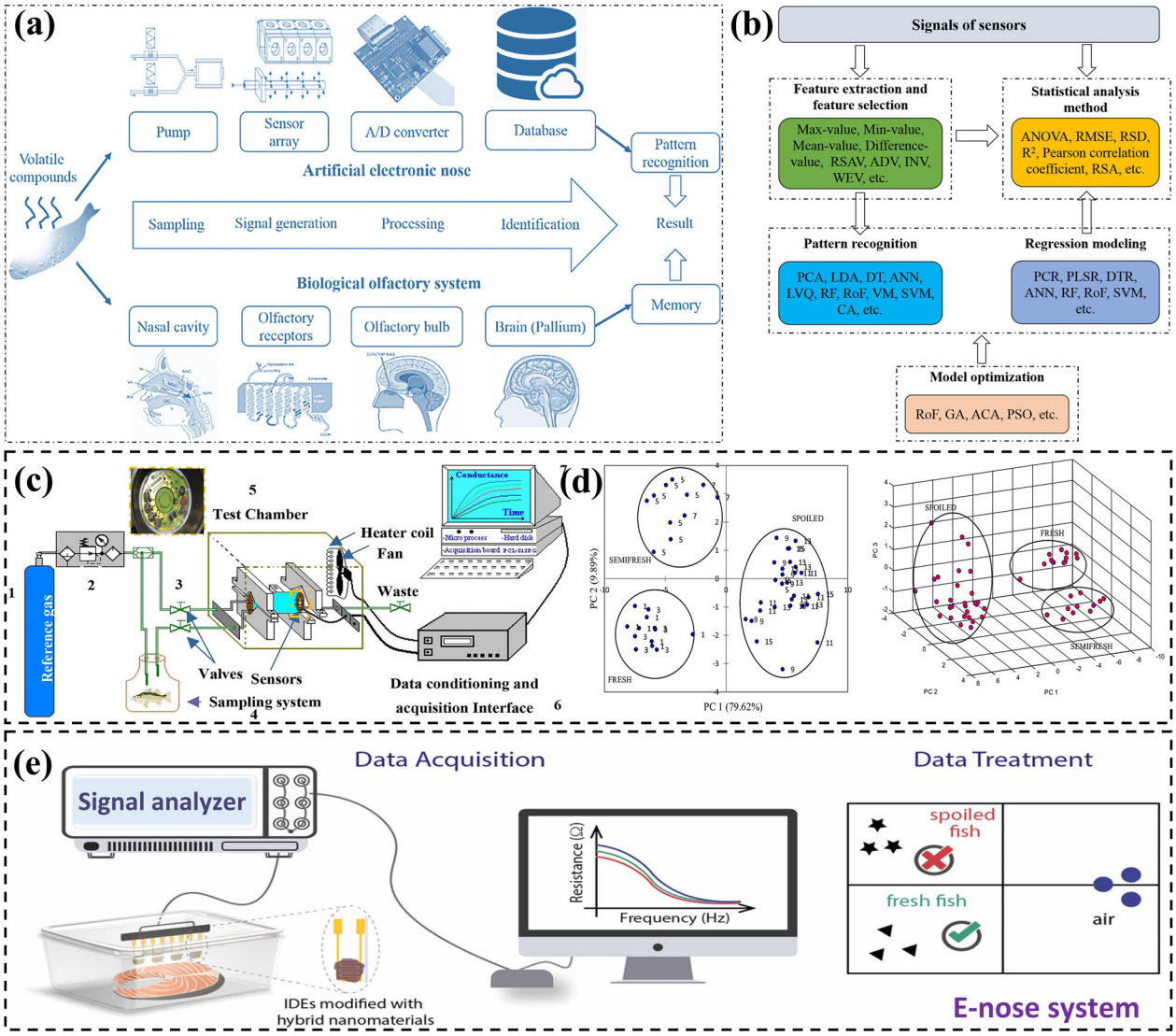

FIGURE 7 (a) The main components of the electronic nose technology and their corresponding biological functions and (b) the analysis scheme of the sensor array signal (Jiang & Liu, 2020). Max-value, the maximum value of the signal; Min-value, the minimum value of the signal; Mean, the average value of the signal; Difference-value, the difference between the maximum and minimum values; RSAV, the relative steady-state response average ADV, mean differential value; INV, integer value; WEV, wavelet energy value; ANOVA, analysis of variance; RMSE, root mean square error; RSD, relative standard deviation; RSA, response surface analysis; PCA, principal component analysis; LDA, Linear Discriminant Analysis; DT, Decision Tree Algorithm; ANN, Artificial Neural Network; LVQ, Learning Vector Quantization; RF, Random Forest Algorithm; RoF, Rotation Forest Algorithm; VM, Voting Method; SVM, Support Vector Machine; CA, Clustering Analysis; PCR, principal component regression; PLSR, partial least squares regression; DTR, decision tree regression; GA, genetic algorithm; ACA, ant colony algorithm; PSO, particle swarm optimization. (c) Schematic diagram of the electronic nose system based on the 7 MOS sensor array. (d) Classification results of fish with different freshness states (fresh, semi-fresh, and rotten) detected by the electronic nose system (Vajdi et al., 2019). (e) Sensor arrays decorated with hybrid nanomaterials: schematic diagram of an electronic nose system for fish spoilage monitoring (Andre et al., 2022)

(MQ2, MQ3, MQ6, MQ9, MQ135) (Leghrib et al., 2020). In this work, a gas-sensing test system was used to obtain the response values, response and recovery time, response area, and other characteristic values of three kinds of fish (Sardine, Cinchard, and Mackerel) at different storage times. By combining the characterization of the sensing responses of five sensors to target fish samples with data processing techniques (PCA), and based on international fish freshness standards, the fish freshness in different storage stages can be distinguished, with a reliability of about 97%. Rivai et al. developed a technique for determining fish quality using semiconductor gas sensor arrays (commercial sensors: H2S-B4, MQ-136, and MQ-137) and neural network (NN) algorithms (Rivai et al., 2019). The 16-bit ADC

ADS1115 module converts analog sensor signals to digital data and then feeds these sensor data to an NN algorithm in the microcontroller. The results showed the rottener the fish, the higher the sensor's response value. The system can identify fresh, semi-fresh, and rotten fish with an 80% success rate. Radi et al. developed an electronic nose using 12 semiconductor gas sensors to detect the tilapia freshness (Radi et al., 2021). The device consisted of semiconductor sensors, sampling module, microcontroller, and signals recording and processing system. The electronic nose was first used to classify 48 fresh tilapia samples and 50 non-fresh tilapia samples. Sensor responses were processed and classified through both PCA and NN patterns. Four methods (absolute data, normalized absolute data, relative data, and normalized relative data) were used to assess the pattern. Among them, the normalized absolute data method showed the highest classification accuracy of 93.88%. Moreover, the freshness of 15 tilapia samples was predicted by a trained NN. The results showed that 60.0% of the samples belonged to the fresh, 33.3% belonged to the spoiled, and 6.7% did not belong to these two categories. Li et al. used a self-developed portable electronic nose based on 10 metal oxide gas sensors to detect and classify the quality of fishmeal (Li, Ren, et al., 2019). The integral value, maximum gradient value, relational steady-state response average value, wavelet energy value, average differential value, and variance value of the sensor response were selected as six low-dimensional feature quantities to study the samples in various storage time. Linear discriminant analysis, PCA, and five kinds of pattern recognitions are used to identify and analyze different quality levels. The results revealed the random forest (RF) model possessed the highest accuracy (93.9%). Vajdi et al. designed a electronic nose based on seven commercial metal oxide gas sensors (TGS 826-NH_3, TGS 825-H_2S, TGS 880-H_2O, TGS 832-Halocarbons, TGS 831-Chlorofluorocarbons, TGS 822-Alcohols, Xylene and Toluene, and TGS 813-combustible gases, Figaro Co, Ltd, Japan) to detect volatiles in fish (Figure 7c) (Vajdi et al., 2019). Fish headspace gas sampling, TVC, and TVB-N analysis were performed simultaneously within 15 storage days to assess the freshness status of fish comprehensively. Thirty-five applicable gases were selected as odor parameters from each headspace sampling test; PCA was used to reduce the 35-dimensional vector to five-dimensional vector. With the five-dimensional vector as the main component, a multilayer perceptron neural network (MLPNN) analysis was performed to clarify the samples as fresh, semi-fresh, and spoiled with the correct rate of 96.87%. The newly introduced hyperdisk model maximum margin optimization classifier (HDM-MOC) achieves 100% accuracy (Figure 7d). In addition, all electronic noses have achieved effective detection of fish spoilage process, and the high correlation coefficient between response parameters and microbial and chemical analysis results proves that the technology can be successfully applied to industrial fish spoilage detection.

In order to simplify the structural design of electronic noses, electronic noses based on fewer nano-metal oxides sensor arrays have been developed. SiO_2:In_2O_3, SiO_2:ZnO, and SiO_2 nanofibers were used as sensing units of electronic noses for detecting NH_3, monomethylamine, and TMA (Figure 7e) (Andre et al., 2022). The complex data on resistive components were evaluated using multidimensional projection techniques. The electronic nose showed good response and precise classification to standard gas and salmon samples (25 g) at different storage times (25 ± 2°C, 0–48 h), indicating its excellent performance in fish spoilage monitoring. Grassi et al. have developed a novel and portable electronic nose system (Mastersense) for assessing fish freshness (Grassi et al., 2019). The sensor array module of the system consists of four commercial metal oxide sensors (GGS 8530, GGS 5430, GGS 2530, and GGS 10530). The Mastersense system tested salmon stored at 4°C (8 days storage, 4 days shelf life). Freshness indicator (green: unspoiled; yellow: acceptable; red: spoiled) was defined in conjunction with analysis of TVCs performed on the same fillet samples, and a classification model was developed using the *K*-nearest neighbor algorithm and partial least squares discriminant analysis. All obtained models have higher prediction accuracy than 83.3%. In addition, the *K*-nearest neighbor model ($p > 0.05$) was found to be more reliable, and the electronic nose is also considered as a convenient strategy for assessing fish freshness.

Table 7 summarizes the MOSR gas sensor array or electronic nose technology targeted at fish freshness detection in the past 5 years, including its sensor array composition, odor recognition type, pattern recognition algorithm, the evaluation accuracy, and other auxiliary verification detection technology. This technology realizes the evaluation, classification, and prediction of fish freshness, and will show broad application prospects in practice.

5 | CHALLENGES AND PROSPECTS

The volatile compound profiles of fish change a lot during storage and processing. Odor property is one of the most important factors that affect the purchasing behavior of consumers. Some volatile compounds such as NH_3 and TMA can be used as indicators of fish freshness. Gas sensors are increasingly important in the qualitative and quantitative evaluation of high-protein foods including fish, among which MOSR gas sensors with the advantages of high response, low cost, miniaturization, and easy integration have been widely studied and proved to possess

TABLE 7 MOSR gas sensor (array), electronic nose, and data processing technology

Type	Product	Gas sensors	Volatile compounds	Application	Pattern recognition and accuracy	Coupled technique	References
Sensors array	Sardines, Chinchard, Mackerel	5 MOS	TMA, ethanol, and hydrogen sulfide	Fish freshness evaluation	PCA and 97%	–	Leghrib et al., 2020
Sensors array	Bubara, Terisi, Mackerel, Mullet, and Fusilier	3 MOS	Hydrogen sulfide and ammonia	Fish freshness and classification	Neural network and 80%.	–	Rivai et al., 2019
Sensors array	Tilapia, Rohu, and Illish	Au/Ag–$SnO_2/SiO_2/Si$	TMA, DMA, ammonia, and hydrogen sulfide	Fish freshness evaluation	–	TVB-N and TVC	Senapati & Sahu, 2020
Electronic nose	Oncorhynchus fish	7 MOS	NH_3, H_2S, halocarbons, chlorofluorocarbons, alcohols, xylene and toluene, and combustible gases	Fish freshness evaluation and classification	PCA, MLPNN, HDMMOC, and 96.87%–100%	TVB-N and TVC	Vajdi et al., 2019
Electronic nose	European plaice and salmon	4 MOS	C_2H_5OH, O_3, VOCs	Fish freshness evaluation and classification	PCA, *K*-NN , PLS-DA, and >83.3%	TVC	Grassi et al., 2019
Electronic nose	Tilapia	12 MOS	NH_3, VOCs	Fish freshness evaluation and classification	PCA, NN, and 93.88%	–	Radi et al., 2021
Electronic nose	Salmon	SiO_2–In_2O_3, SiO_2–ZnO, and SiO_2	NH_3, TMA, and methylamine	Fish freshness evaluation and classification	PCA and IDMAP	–	Andre et al., 2022
Electronic nose	Mahi-mahi, croaker, red snapper, and weakfish	8 MOS	NH_3, H_2S, hydrocarbons, and total volatile organic carbon	Fish freshness evaluation, classification, and prediction	PCA, SVM, and 97%–100%	–	Karunathilaka et al., 2021
Electronic nose	Tilapia	18 MOS	NH_3, H_2S, amines, hydrocarbons, propane/butane, and alcohols	Fish freshness evaluation, classification, and prediction	PCA, RBFNN, and >90%	TVB-N, TVC, GC–MS, *K*-value, and sensory score	Shi et al., 2018

Abbreviations: IDMAP, nonlinear Interactive Document Mapping; *K*-NN, *K*-nearest neighbors; PLS-DA, partial least square-discriminant analysis; RBFNN, radial basis function neural networks.

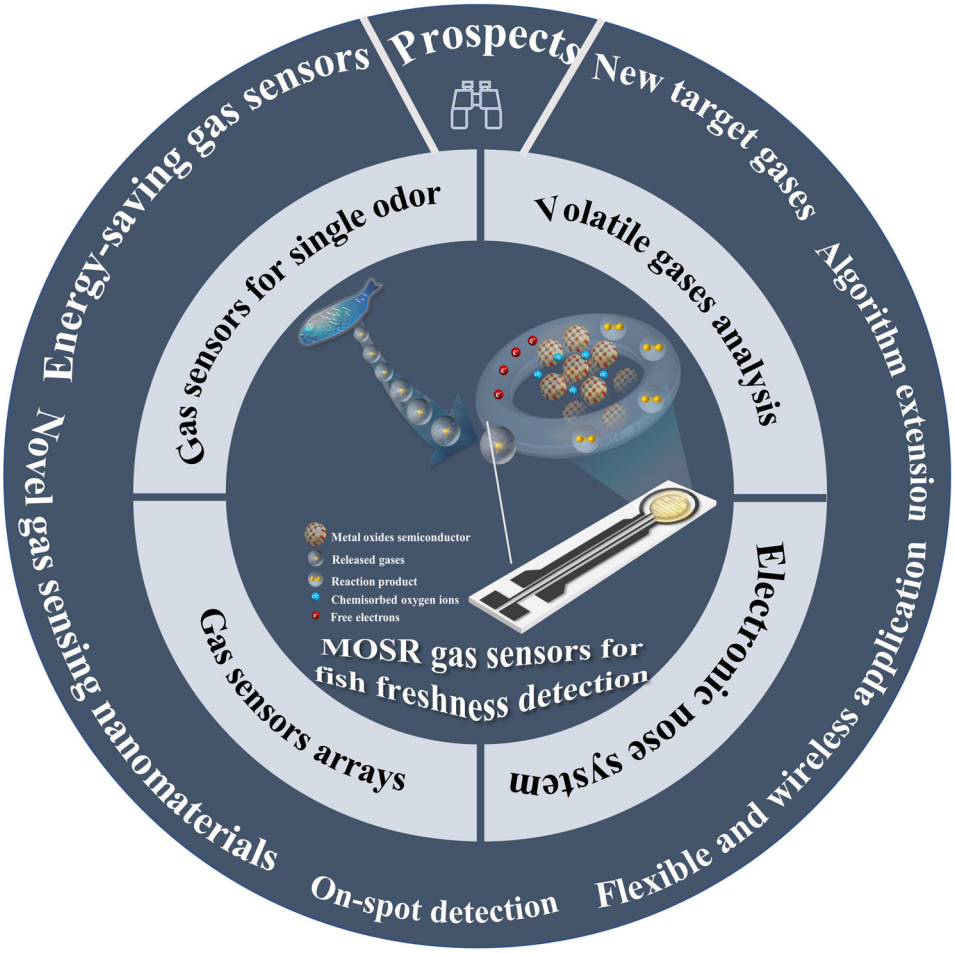

FIGURE 8 An overview of MOSR-based gas sensors for fish freshness detection and the prospective and possible solutions for the faced challenges by this technology

large practical application potential. As sown in Figure 8, the current research trends and practical application of MOSR gas sensors are discussed, and the corresponding gas sensor arrays or electronic nose coupling with different data processing methods are also summarized in this review. Furthermore, there are lots of released VOCs (alcohols, ketones, and aldehydes) from rotten fish, which can be recommended as the supplemented biomarker indicators to assess the fish freshness. Hence, studying the released gas concentration range and effective gas-sensing materials for alcohols, ketones, and aldehydes will be the potential research field.

Although the rapid detection technology of fish freshness based on metal oxide gas sensors (array) or electronic nose shows good performance, this technology still faces many challenges (sampling system, sensing module, and pattern recognition technology). The specific challenges and possible solutions are listed below.

5.1 | High operating temperature of the metal oxide gas sensors and the complexity of the device structure

When gas molecules are adsorbed on the gas-sensing layer, a redox reaction will occur at the gas–solid interface. Still, the self-activation energy is not enough for an effective reaction. Additional energy (high-temperature heating or light) is required to promote the reaction rate and overcome the energy potential barrier to obtain satisfactory gas-sensing performance such as sensitivity. However, high operating temperature or light activation will not only lead to a second grain growth (weakening gas-sensing performance) and high power consumption, but also increase the design complexity of the device structure. To solve such problems, the development of new gas-sensing materials will be a feasible solution. Among them, the development of two-dimensional materials (transition metal selenium

compounds, black phosphorus) provides new options for room-temperature sensors. Therefore, effectively coupling them with metal oxides to lower the operating temperature and obtain high performance may be a future research focus. Therefore, the research on the above new gas sensors will be of great significance to the development of microminiaturized array structure and electronic nose technology.

5.2 | Insufficient detection limit of the MOSR gas sensor

Currently, the detection accuracy of electronic nose based on metal oxide gas sensors is ppm or sub-ppm level. It is difficult to meet the detection requirements of lower concentrations of volatile gases, which will reduce its application ability in the field of freshness detection. In addition to the two commonly used methods of designing new material nanostructures and introducing enhanced phases, it is also necessary to develop new gas-sensing materials and performance enhancement strategies employing theoretical simulations and experimental demonstrations based on the gas-sensing mechanism.

5.3 | Baseline drift of metal oxide gas sensors

Due to changes in environmental conditions such as temperature, humidity, and the presence of interfering gases, the baseline of the sensor will drift, and the sensing signal needs to be calibrated. Besides adding additional temperature and humidity sensors inside the electronic nose system to calibrate the drift, developing sensing materials with a high signal-to-noise ratio or covering the sensing materials with MOF or hydrophobic coatings can effectively reduce the influence of interference gas and ambient humidity changes, thus improving gas selectivity and detection accuracy.

5.4 | Limitations of the pattern recognition algorithms

Gas sensing technology will develop from single gas detection to multi-index detection. The traditional gas signal processing methods will also extend into intelligent data processing methods, such as new feature extraction algorithms that can perform complex mapping, fuzzy set theory, and other signal processing techniques that can mimic the human mind. In addition, regression algorithms for building freshness prediction models also need further development, and machine deep learning will be a viable option.

5.5 | Limitations of application scenarios

It is the future development trend to transform the array or the electronic nose technology based on metal oxide sensors from laboratory detection to various application scenarios, such as long-distance transportation, smart food packaging, and real-time market monitoring. However, due to the limitations of the existing sensing device technology, such as the lack of flexible structure, external power supply, low degree of visualization, and difficulty in portability, the further development of the detection technology is limited. To overcome such problems, designing flexible circuits and wearable devices, self-powered sensors, and smart sensing devices based on Bluetooth, wireless, or NFC communication modes will be the focus of future research.

5.6 | Lacked research on MOSR gas sensor behaviors under a practical environment

The existing works on MOSR gas sensors for fish freshness detection have commonly used the separated fish sample stored at certain conditions as a target. Though the storage environment was simulated in temperature and humidity, the fish in the whole supply chain (transportation and market shelves stage) is necessary to be detected to verify the real practical potentials of MOSR gas sensors, that is, the on-spot detection. This may be the future research trend for the MOSR gas sensors arrays or the electronic nose.

AUTHOR CONTRIBUTIONS

Kaidi Wu: Investigation; Visualization; Writing – original draft; Writing – review & editing; Methodology; Conceptualization; Data curation; Software. **Marc Debliquy:** Formal analysis; Supervision; Resources; Writing – review & editing; Validation. **Chao Zhang:** Conceptualization; Funding acquisition; Resources; Supervision; Project administration; Writing – review & editing; Methodology; Formal analysis; Validation; Visualization.

ACKNOWLEDGMENTS

This work was financially supported by the National Natural Science Foundation of China (Grant no. 51872254), the Outstanding Youth of Jiangsu Province of China (Grant no. BK20211548), the National Key Research and Development Program of China (Grant no. 2017YFE0115900),

and the Excellent Doctoral Dissertation Fund of Yangzhou University (2021_06).

CONFLICT OF INTEREST

The authors declare no conflict of interest.

ORCID

Kaidi Wu https://orcid.org/0000-0001-8683-8928
Chao Zhang https://orcid.org/0000-0003-2346-6770

REFERENCES

Andre, R. S., Facure, M. H. M., Mercante, L. A., & Correa, D. S. (2022). Electronic nose based on hybrid free-standing nanofibrous mats for meat spoilage monitoring. *Sensors and Actuators B: Chemical*, *353*, 131114. https://doi.org/10.1016/j.snb.2021.131114

Bai, S., Han, J., Han, N., Zhang, K., Sun, J., Sun, L., Luo, R., Li, D., & Chen, A. (2020). An α-Fe_2O_3/NiO p-n hierarchical heterojunction for the sensitive detection of triethylamine. *Inorganic Chemistry Frontiers*, *7*(7), 1532–1539. https://doi.org/10.1039/C9QI01548E

Bernardo, Y. A. A., Rosario, D. K. A., Delgado, I. F., & Conte-Junior, C. A. (2020). Fish Quality Index Method: Principles, weaknesses, validation, and alternatives - A review. *Comprehensive Reviews in Food Science and Food Safety*, *19*(5), 2657–2676. https://doi.org/10.1111/1541-4337.12600

Bruce, J., Bosnick, K., & Kamali Heidari, E. (2022). Pd-decorated ZnO nanoflowers as a promising gas sensor for the detection of meat spoilage. *Sensors and Actuators B: Chemical*, *355*, 131316. https://doi.org/10.1016/j.snb.2021.131316

Chang, L.-Y., Chuang, M.-Y., Zan, H.-W., Meng, H.-F., Lu, C.-J., Yeh, P.-H., & Chen, J.-N. (2017). One-minute fish freshness evaluation by testing the volatile amine gas with an ultrasensitive porous-electrode-capped organic gas sensor system. *ACS Sensors*, *2*(4), 531–539. https://doi.org/10.1021/acssensors.6b00829

Chen, G., Chu, X., Qiao, H., Ye, M., Chen, J., Gao, C., & Guo, C.-Y. (2018). Thickness controllable single-crystal WO_3 nanosheets: Highly selective sensor for triethylamine detection at room temperature. *Materials Letters*, *226*, 59–62. https://doi.org/10.1016/j.matlet.2018.05.022

Chen, Y., Li, Y., Feng, B., Wu, Y., Zhu, Y., & Wei, J. (2022). Self-templated synthesis of mesoporous Au-ZnO nanospheres for seafood freshness detection. *Sensors and Actuators B: Chemical*, *360*, 131662. https://doi.org/10.1016/j.snb.2022.131662

Cheng, J.-H., Dai, Q., Sun, D.-W., Zeng, X.-A., Liu, D., & Pu, H.-B. (2013). Applications of non-destructive spectroscopic techniques for fish quality and safety evaluation and inspection. *Trends in Food Science & Technology*, *34*(1), 18–31. https://doi.org/10.1016/j.tifs.2013.08.005

Cheng, J.-H., Sun, D.-W., Han, Z., & Zeng, X.-A. (2014). Texture and structure measurements and analyses for evaluation of fish and fillet freshness quality: A review. *Comprehensive Reviews in Food Science and Food Safety*, *13*(1), 52–61. https://doi.org/10.1111/1541-4337.12043

Cheng, J.-H., Sun, D.-W., Zeng, X.-A., & Liu, D. (2015). Recent advances in methods and techniques for freshness quality determination and evaluation of fish and fish fillets: A review. *Critical Reviews in Food Science and Nutrition*, *55*(7), 1012–1225. https://doi.org/10.1080/10408398.2013.769934

Cho, Y. H., Kang, Y. C., & Lee, J.-H. (2013). Highly selective and sensitive detection of trimethylamine using WO_3 hollow spheres prepared by ultrasonic spray pyrolysis. *Sensors and Actuators B: Chemical*, *176*, 971–977. https://doi.org/10.1016/j.snb.2012.10.044

Chou, T.-C., Chang, C.-H., Lee, C., & Liu, W.-C. (2019). Ammonia sensing characteristics of a tungsten trioxide thin-film-based sensor. *IEEE Transactions on Electron Devices*, *66*(1), 696–701. https://doi.org/10.1109/TED.2018.2882737

Chu, X., Wang, J., Gao, Q., Wang, Y., Liang, S., & Bai, L. (2020). High selectivity trimethylamine sensors based on graphene-$NiGa_2O_4$ nanocomposites prepared by hydrothermal method. *Physica E: Low-dimensional Systems and Nanostructures*, *118*, 113788. https://doi.org/10.1016/j.physe.2019.113788

Duflos, G., Coin, V. M., Cornu, M., Antinelli, J.-F., & Malle, P. (2006). Determination of volatile compounds to characterize fish spoilage using headspace/mass spectrometry and solid-phase microextraction/gas chromatography/mass spectrometry. *Journal of the Science of Food and Agriculture*, *86*(4), 600–611. https://doi.org/10.1002/jsfa.2386

El Barbri, N., Amari, A., Vinaixa, M., Bouchikhi, B., Correig, X., & Llobet, E. (2007). Building of a metal oxide gas sensor-based electronic nose to assess the freshness of sardines under cold storage. *Sensors and Actuators B: Chemical*, *128*(1), 235–244. https://doi.org/10.1016/j.snb.2007.06.007

Fan, Y., Xu, Y., Wang, Y., & Sun, Y. (2021). Fabrication and characterization of Co-doped ZnO nanodiscs for selective TEA sensor applications with high response, high selectivity and ppb-level detection limit. *Journal of Alloys and Compounds*, *876*, 160170. https://doi.org/10.1016/j.jallcom.2021.160170

Feng, B., Wu, Y., Chen, Y., Yuan, K., Yue, Q., Deng, Y., & Wei, J. (2022). Polyphenol-mediated synthesis of mesoporous Au–In_2O_3 nanospheres for room-temperature detection of triethylamine. *ACS Applied Nano Materials*, *5*(7), 9688–9697. https://doi.org/10.1021/acsanm.2c01927

Feng, B., Wu, Y., Ren, Y., Chen, Y., Yuan, K., Deng, Y., & Wei, J. (2022). Self-template synthesis of mesoporous Au-SnO_2 nanospheres for low-temperature detection of triethylamine vapor. *Sensors and Actuators B: Chemical*, *356*, 131358. https://doi.org/10.1016/j.snb.2021.131358

Galstyan, V., Bhandari, M., Sberveglieri, V., Sberveglieri, G., & Comini, E. (2018). Metal oxide nanostructures in food applications: Quality control and packaging. *Chemosensors*, *6*(2), 16. https://doi.org/10.3390/chemosensors6020016

Galstyan, V., Ponzoni, A., Kholmanov, I., Natile, M. M., Comini, E., & Sberveglieri, G. (2020). Highly sensitive and selective detection of dimethylamine through Nb-doping of TiO_2 nanotubes for potential use in seafood quality control. *Sensors and Actuators B: Chemical*, *303*, 127217. https://doi.org/10.1016/j.snb.2019.127217

Ganesan, S., Muruganandham, A., Mounasamy, V., Kannan, V. P., & Madanagurusamy, S. (2020). Highly selective dimethylamine sensing performance of TiO_2 thin films at room temperature. *Journal of Nanoscience and Nanotechnology*, *20*(5), 3131–3139. https://doi.org/10.1166/jnn.2020.17199

Ghaly, A. E., Dave, D., Budge, S., & Brooks, M. S. (2010). Fish spoilage mechanisms and preservation techniques: Review. *American Journal of Applied Sciences*, *7*(7), 859–877. https://doi.org/10.3844/ajassp.2010.859.877

Grassi, B., Opizzio, N., & Buratti, S. (2019). Meat and fish freshness assessment by a portable and simplified electronic nose

system (Mastersense). *Sensors*, *19*(14), 3225. https://doi.org/10.3390/s19143225

Grassi, S., Benedetti, S., Magnani, L., Pianezzola, A., & Buratti, S. (2022). Seafood freshness: E-nose data for classification purposes. *Food Control*, *138*, 108994. https://doi.org/10.1016/j.foodcont.2022.108994

Gu, F., Cui, Y., Han, D., Hong, S., Flytzani-Stephanopoulos, M., & Wang, Z. (2019). Atomically dispersed Pt (II) on WO_3 for highly selective sensing and catalytic oxidation of triethylamine. *Applied Catalysis B: Environmental*, *256*, 117809. https://doi.org/10.1016/j.apcatb.2019.117809

Gu, Q., Fu, L., Wang, Y., & Lin, J. (2013). Identification and characterization of extracellular cyclic dipeptides as quorum-sensing signal molecules from *Shewanella baltica*, the specific spoilage organism of *Pseudosciaena crocea* during 4°C storage. *Journal of Agricultural and Food Chemistry*, *61*(47), 11645–11652. https://doi.org/10.1021/jf403918x

Güney, S., & Atasoy, A. (2015). Study of fish species discrimination via electronic nose. *Computers and Electronics in Agriculture*, *119*, 83–91. https://doi.org/10.1016/j.compag.2015.10.005

Hammond, J., Marquis, B., Michaels, R., Oickle, B., Segee, B., Vetelino, J., Bushway, A., Camire, M. E., & Davis-Dentici, K. (2002). A semiconducting metal-oxide array for monitoring fish freshness. *Sensors and Actuators B: Chemical*, *84*(2), 113–122. https://doi.org/10.1016/S0925-4005(02)00011-4

Han, F., Huang, X., Teye, E., Gu, H., Dai, H., & Yao, L. (2014). A nondestructive method for fish freshness determination with electronic tongue combined with linear and non-linear multivariate algorithms. *Czech Journal of Food Sciences*, *32*(6), 532–537. https://doi.org/10.17221/88/2014-CJFS

Hassoun, A., & Karoui, R. (2017). Quality evaluation of fish and other seafood by traditional and nondestructive instrumental methods: Advantages and limitations. *Critical Reviews in Food Science and Nutrition*, *57*(9), 1976–1998. https://doi.org/10.1080/10408398.2015.1047926

Heising, J. K., van Boekel, M. A. J. S., & Dekker, M. (2014). Mathematical models for the trimethylamine (TMA) formation on packed cod fish fillets at different temperatures. *Food Research International*, *56*, 272–278. https://doi.org/10.1016/j.foodres.2014.01.011

Hu, C., Yu, L., Li, S., Yin, M., Du, H., & Li, H. (2022). Sacrificial template triggered to synthesize hollow nanosheet-assembled Co_3O_4 microtubes for fast triethylamine detection. *Sensors and Actuators B: Chemical*, *355*, 131246. https://doi.org/10.1016/j.snb.2021.131246

Hu, Q., He, J., Chang, J., Gao, J., Huang, J., & Feng, L. (2020). Needle-shaped WO_3 nanorods for triethylamine gas sensing. *ACS Applied Nano Materials*, *3*(9), 9046–9054. https://doi.org/10.1021/acsanm.0c01731

Hu, X., Zhu, Z., Chen, C., Wen, T., Zhao, X., & Xie, L. (2017). Highly sensitive H_2S gas sensors based on Pd-doped CuO nanoflowers with low operating temperature. *Sensors and Actuators B: Chemical*, *253*, 809–817. https://doi.org/10.1016/j.snb.2017.06.183

Huan, Y., Wu, K., Li, C., Liao, H., Debliquy, M., & Zhang, C. (2020). Micro-nano structured functional coatings deposited by liquid plasma spraying. *Journal of Advanced Ceramics*, *9*(5), 517–534. https://doi.org/10.1007/s40145-020-0402-9

Huang, Y.-Z., Liu, Y., Jin, Z., Cheng, Q., Qian, M., Zhu, B.-W., & Dong, X.-P. (2021). Sensory evaluation of fresh/frozen mackerel products: A review. *Comprehensive Reviews in Food Science and Food Safety*, *20*(4), 3504–3530. https://doi.org/10.1111/1541-4337.12776

Haouet, M. N. (2001). *Istituto Zooprofilattico Sperimentale dell'Umbria e delle Marche - Speciale Prodotti Ittici*. https://www.spvet.it/arretrati/numero_8_9/ittici.html#2. Accessed 9 October 2022.

Jia, W., Liang, G., Jiang, Z., & Wang, J. (2019). Advances in electronic nose development for application to agricultural products. *Food Analytical Methods*, *12*(10), 2226–2240. https://doi.org/10.1007/s12161-019-01552-1

Jia, W., Liang, G., Wang, Y., & Wang, J. (2018). Electronic noses as a powerful tool for assessing meat quality: A mini review. *Food Analytical Methods*, *11*(10), 2916–2924. https://doi.org/10.1007/s12161-018-1283-1

Jiang, S., & Liu, Y. (2020). Gas sensors for volatile compounds analysis in muscle foods: A review. *TrAC Trends in Analytical Chemistry*, *126*, 115877. https://doi.org/10.1016/j.trac.2020.115877

Johnson, J., Atkin, D., Lee, K., Sell, M., & Chandra, S. (2019). Determining meat freshness using electrochemistry: Are we ready for the fast and furious? *Meat Science*, *150*, 40–46. https://doi.org/10.1016/j.meatsci.2018.12.002

Ju, D.-X., Xu, H.-Y., Qiu, Z.-W., Zhang, Z.-C., Xu, Q., & Zhang, J. (2015). Near room temperature, fast-response, and highly sensitive triethylamine sensor assembled with Au-loaded ZnO/SnO_2 core–shell nanorods on flat alumina substrates. *ACS Applied Materials & Interfaces*, *7*(34), 19163–19171. https://doi.org/10.1021/acsami.5b04904

Kademi, H. I., Ulusoy, B. H., & Hecer, C. (2019). Applications of miniaturized and portable near infrared spectroscopy (NIRS) for inspection and control of meat and meat products. *Food Reviews International*, *35*(3), 201–220. https://doi.org/10.1080/87559129.2018.1514624

Karunathilaka, S. R., Ellsworth, Z., & Yakes, B. J. (2021). Detection of decomposition in mahi-mahi, croaker, red snapper, and weakfish using an electronic-nose sensor and chemometric modeling. *Journal of Food Science*, *86*(9), 4148–4158. https://doi.org/10.1111/1750-3841.15878

Katiyo, W., de Kock, H. L., Coorey, R., & Buys, E. M. (2020). Sensory implications of chicken meat spoilage in relation to microbial and physicochemical characteristics during refrigerated storage. *LWT - Food Science and Technology*, *128*, 109468. https://doi.org/10.1016/j.lwt.2020.109468

Kent, M., Oehlenschlager, J., Mierke-Klemeyer, S., Manthey-Karl, M., Knöchel, R., Daschner, F., & Schimmer, O. (2004). A new multivariate approach to the problem of fish quality estimation. *Food Chemistry*, *87*(4), 531–535. https://doi.org/10.1016/j.foodchem.2004.01.004

Kim, J.-S., Kim, K. B., Li, H.-Y., Na, C. W., Lim, K., Moon, Y. K., Yoona, J. W., & Lee, J.-H. (2021). Pure and Pr-doped $Ce_4W_9O_{33}$ with superior hydroxyl scavenging ability: Humidity-independent oxide chemiresistors. *Journal of Materials Chemistry A*, *9*(30), 16359–16369. https://doi.org/10.1039/D1TA02618F

Kim, T.-H., Kim, K. B., & Lee, J.-H. (2019). Highly sensitive and selective trimethylamine sensor using yolk-shell structured Mo-doped Co_3O_4 spheres. *Journal of Sensor Science and Technology*, *28*(5), 271–276. https://doi.org/10.5369/JSST.2019.28.5.271

Kutsanedzie, F. Y. H., Guo, Z., & Chen, Q. (2019). Advances in nondestructive methods for meat quality and safety monitoring. *Food Reviews International*, *35*(6), 536–562. https://doi.org/10.1080/87559129.2019.1584814

Leghrib, R., Aantri, Y., Sanchez, J. B., Berger, F., & Kaaya, A. (2020). Assessing the freshness of Agadir blue fish using a metal oxide

gas sensing array. *Materials Today: Proceedings*, *22*, 1–5. https://doi.org/10.1016/j.matpr.2019.08.054

Li, H., Chu, S., Ma, Q., Fang, Y., Wang, J., Che, Q., Wang, G., & Yang, P. (2019). Novel construction of morphology-tunable C–N/SnO_2/ZnO/Au microspheres with ultrasensitivity and high selectivity for triethylamine under various temperature detections. *ACS Applied Materials & Interfaces*, *11*(8), 8601–8611. https://doi.org/10.1021/acsami.8b22357

Li, H.-Y., Lee, C.-S., Kim, D. H., & Lee, J.-H. (2018). Flexible room-temperature NH_3 sensor for ultrasensitive, selective, and humidity-independent gas detection. *ACS Applied Materials & Interfaces*, *10*(33), 27858–27867. https://doi.org/10.1021/acsami.8b09169

Li, P., Geng, J., Li, H., & Niu, Z. (2020). Fish meal freshness detection by GBDT based on a portable electronic nose system and HS-SPME–GC–MS. *European Food Research and Technology*, *246*(6), 1129–1140. https://doi.org/10.1007/s00217-020-03462-7

Li, P., Ren, Z., Shao, K., Tan, H., & Niu, Z. (2019). Research on distinguishing fish meal quality using different characteristic parameters based on electronic nose technology. *Sensors*, *19*(9), 2146. https://doi.org/10.3390/s19092146

Li, Q., Zhang, L., & Luo, Y. (2018). Changes in microbial communities and quality attributes of white muscle and dark muscle from common carp (*Cyprinus carpio*) during chilled and freeze-chilled storage. *Food Microbiology*, *73*, 237–244. https://doi.org/10.1016/j.fm.2018.01.011

Li, Y., Lu, Y.-L., Wu, K.-D., Zhang, D.-Z., Debliquy, M., & Zhang, C. (2021). Microwave-assisted hydrothermal synthesis of copper oxide-based gas-sensitive nanostructures. *Rare Metals*, *40*(6), 1477–1493. https://doi.org/10.1007/s12598-020-01557-4

Li, Y., Liu, J., Zhang, J., Liang, X., Zhang, X., & Qi, Q. (2020). Deposition of In_2O_3 nanofibers on polyimide substrates to construct high-performance and flexible trimethylamine sensor. *Chinese Chemical Letters*, *31*(8), 2142–2144. https://doi.org/10.1016/j.cclet.2019.11.048

Li, Y., Li, K., Luo, Y., Liu, B., Wang, H., Gao, L., & Duan, G. (2020). Synthesis of Co_3O_4/ZnO nano-heterojunctions by one-off processing ZIF-8@ZIF-67 and their gas-sensing performances for trimethylamine. *Sensors and Actuators B: Chemical*, *308*, 127657. https://doi.org/10.1016/j.snb.2020.127657

Li, Z., Song, P., Yang, Z., & Wang, Q. (2018). In situ formation of one-dimensional $CoMoO_4$/MoO_3 heterojunction as an effective trimethylamine gas sensor. *Ceramics International*, *44*(3), 3364–3370. https://doi.org/10.1016/j.ceramint.2017.11.126

Liu, B., Li, K., Luo, Y., Gao, L., & Duan, G. (2021). Sulfur spillover driven by charge transfer between AuPd alloys and SnO_2 allows high selectivity for dimethyl disulfide gas sensing. *Chemical Engineering Journal*, *420*, 129881. https://doi.org/10.1016/j.cej.2021.129881

Liu, L., Fu, S., Lv, X., Yue, L., Fan, L., Yu, H., Gao, X., Zhu, W., Zhang, W., Li, X., & Zhu, W. (2020). A gas sensor with Fe_2O_3 nanospheres based on trimethylamine detection for the rapid assessment of spoilage degree in fish. *Frontiers in Bioengineering and Biotechnology*, *8*, 567584. https://doi.org/10.3389/fbioe.2020.567584

Liu, M., Song, P., Zhong, X., Yang, Z., & Wang, Q. (2020). Facile synthesis of Au-decorated α-Fe_2O_3/rGO ternary hybrid structure nanocomposites for enhanced triethylamine gas-sensing properties. *Journal of Materials Science: Materials in Electronics*, *31*(24), 22713–22726. https://doi.org/10.1007/s10854-020-04796-4

Liu, Y., Guo, R., Yuan, K., Gu, M., Lei, M., Yuan, C., Gao, M., Ai, Y., Liao, Y., Yang, X., Ren, Y., Zou, Y., & Deng, Y. (2022). Engineering pore walls of mesoporous tungsten oxides via Ce doping for the development of high-performance smart gas sensors. *Chemistry of Materials*, *34*(5), 2321–2332. https://doi.org/10.1021/acs.chemmater.1c04216

Ma, Q., Chu, S., Li, H., Guo, J., Zhang, Q., & Lin, Z. (2021). Flower-like In_2O_3/ZnO heterostructure with accelerated multi-orientation electron transport mechanism for superior triethylamine detection. *Applied Surface Science*, *569*, 151074. https://doi.org/10.1016/j.apsusc.2021.151074

Meng, D., Liu, D., Wang, G., Shen, Y., San, X., Si, J., & Meng, F. (2019). In-situ growth of ordered Pd-doped ZnO nanorod arrays on ceramic tube with enhanced trimethylamine sensing performance. *Applied Surface Science*, *463*, 348–356. https://doi.org/10.1016/j.apsusc.2018.08.228

Meng, D., Si, J., Wang, M., Wang, G., Shen, Y., San, X., & Meng, F. (2020). In-situ growth of V_2O_5 flower-like structures on ceramic tubes and their trimethylamine sensing properties. *Chinese Chemical Letters*, *31*(8), 2133–2136. https://doi.org/10.1016/j.cclet.2019.12.021

Meng, F., Zheng, H., Sun, Y., Li, M., & Liu, J. (2017). Trimethylamine sensors based on Au-modified hierarchical porous single-crystalline ZnO nanosheets. *Sensors*, *17*(7), 1478. https://doi.org/10.3390/s17071478

Miao, J., Chen, C., & Lin, J. Y. S. (2020). Humidity independent hydrogen sulfide sensing response achieved with monolayer film of CuO nanosheets. *Sensors and Actuators B: Chemical*, *309*, 127785. https://doi.org/10.1016/j.snb.2020.127785

Mitsubayashi, K., Kubotera, Y., Yano, K., Hashimoto, Y., Kon, T., Nakakura, S., Nishi, Y., & Endo, H. (2004). Trimethylamine biosensor with flavin-containing monooxygenase type 3 (FMO3) for fish-freshness analysis. *Sensors and Actuators B: Chemical*, *103*(1), 463–467. https://doi.org/10.1016/j.snb.2004.05.006

Miyasaki, T., Hamaguchi, M., & Yokoyama, S. (2011). Change of volatile compounds in fresh fish meat during ice storage. *Journal of Food Science*, *76*(9), C1319–C1325. https://doi.org/10.1111/j.1750-3841.2011.02388.x

Nevigato, T., Masci, M., Casini, I., Caproni, R., & Orban, E. (2018). Trimethylamine as a freshness indicator for seafood stored in ice: Analysis by GC-FID of four species caught in the Tyrrhenian Sea. *Italian Journal of Food Science*, *30*(3). https://doi.org/10.14674/IJFS-1092

Olafsdóttir, G., Martinsdóttir, E., Oehlenschläger, J., Dalgaard, P., Jensen, B., Undeland, I., Mackie, I. M., Henehan, G., Nielsen, J., & Nilsen, H. (1997). Methods to evaluate fish freshness in research and industry. *Trends in Food Science & Technology*, *8*(8), 258–265. https://doi.org/10.1016/S0924-2244(97)01049-2

Olafsdottir, G., Nesvadba, P., Di Natale, C., Careche, M., Oehlenschläger, J., Tryggvadóttir, S. V., Schubring, R., Kroeger, M., Heia, K., Esaiassen, M., Macagnano, A., & Jørgensen, B. M. (2004). Multisensor for fish quality determination. *Trends in Food Science & Technology*, *15*(2), 86–93. https://doi.org/10.1016/j.tifs.2003.08.006

Ólafsson, R., Martinsdottir, E., Ólafsdottir, G., Sigfusson, P. I., & Gardner, J. W. (1992). Monitoring of fish freshness using tin oxide sensors. In J. W. Gardner & P. N. Bartlett (Eds.), *Sensors and sensory systems for an electronic nose* (pp. 257–272). Springer Netherlands. https://doi.org/10.1007/978-94-015-7985-8_16

Pandeeswari, R., Sonia, T., Balamurugan, D., & Jeyaprakash, B. G. (2022). Highly selective dimethylamine vapour sensors based on spray deposited β-Bi_2O_3 nanospheres at low temperature. *Sensing and Imaging*, *23*(1), 1. https://doi.org/10.1007/s11220-021-00371-1

Park, S. H., Kim, B.-Y., Jo, Y. K., Dai, Z., & Lee, J.-H. (2020). Chemiresistive trimethylamine sensor using monolayer SnO_2 inverse opals decorated with Cr_2O_3 nanoclusters. *Sensors and Actuators B: Chemical*, *309*, 127805. https://doi.org/10.1016/j.snb.2020.127805

Parlapani, F. F., Mallouchos, A., Haroutounian, S. A., & Boziaris, I. S. (2017). Volatile organic compounds of microbial and non-microbial origin produced on model fish substrate un-inoculated and inoculated with gilt-head sea bream spoilage bacteria. *LWT - Food Science and Technology*, *78*, 54–62. https://doi.org/10.1016/j.lwt.2016.12.020

Pei, X., Hu, J., Song, H., Zhang, L., & Lv, Y. (2021). Ratiometric cataluminescence sensor of amine vapors for discriminating meat spoilage. *Analytical Chemistry*, *93*(17), 6692–6697. https://doi.org/10.1021/acs.analchem.1c00034

Pereira, P. F. M., de Sousa Picciani, P. H., Calado, V., & Tonon, R. V. (2021). Electrical gas sensors for meat freshness assessment and quality monitoring: A review. *Trends in Food Science & Technology*, *118*, 36–44. https://doi.org/10.1016/j.tifs.2021.08.036

Pons-Sánchez-Cascado, S., Vidal-Carou, M. C., Mariné-Font, A., & Veciana-Nogués, M. T. (2005). Influence of the freshness grade of raw fish on the formation of volatile and biogenic amines during the manufacture and storage of vinegar-marinated anchovies. *Journal of Agricultural and Food Chemistry*, *53*(22), 8586–8592. https://doi.org/10.1021/jf050867m

Prabhakar, P. K., Vatsa, S., Srivastav, P. P., & Pathak, S. S. (2020). A comprehensive review on freshness of fish and assessment: Analytical methods and recent innovations. *Food Research International*, *133*, 109157. https://doi.org/10.1016/j.foodres.2020.109157

Radi, R., Wahyudi, E., Adhityamurti, M. D., Putro, J. P. L. Y., Barokah, B., & Rohmah, D. N. (2021). Freshness assessment of tilapia fish in traditional market based on an electronic nose. *Bulletin of Electrical Engineering and Informatics*, *10*(5), 2466–2476. https://doi.org/10.11591/eei.v10i5.3111

Rivai, M., Misbah, Attamimi, M., Firdaus, M. H., Tasripan, & Tukadi. (2019). *Fish quality recognition using electrochemical gas sensor array and neural network*. Presented at the 2019 International Conference on Computer Engineering, Network, and Intelligent Multimedia (CENIM), Surabaya, Indonesia. https://doi.org/10.1109/CENIM48368.2019.8973369

Schweizer-Berberich, P.-M., Vaihinger, S., & Göpel, W. (1994). Characterisation of food freshness with sensor arrays. *Sensors and Actuators B: Chemical*, *18*(1), 282–290. https://doi.org/10.1016/0925-4005(94)87095-0

Semeano, A. T. S., Maffei, D. F., Palma, S., Li, R. W. C., Franco, B. D. G. M., Roque, A. C. A., & Gruber, J. (2018). Tilapia fish microbial spoilage monitored by a single optical gas sensor. *Food Control*, *89*, 72–76. https://doi.org/10.1016/j.foodcont.2018.01.025

Senapati, M., & Sahu, P. P. (2020). Onsite fish quality monitoring using ultra-sensitive patch electrode capacitive sensor at room temperature. *Biosensors and Bioelectronics*, *168*, 112570. https://doi.org/10.1016/j.bios.2020.112570

Shang, Y., Shi, R., Cui, Y., Che, Q., Wang, J., & Yang, P. (2020). Urchin-like $WO_{2.72}$ microspheres decorated with Au and PdO nanoparticles for the selective detection of trimethylamine. *ACS Applied Nano Materials*, *3*(6), 5554–5564. https://doi.org/10.1021/acsanm.0c00827

Shen, J., Xu, S., Zhao, C., Qiao, X., Liu, H., Zhao, Y., Wei, J., & Zhu, Y. (2021). Bimetallic Au@Pt nanocrystal sensitization mesoporous α-Fe_2O_3 hollow nanocubes for highly sensitive and rapid detection of fish freshness at low temperature. *ACS Applied Materials & Interfaces*, *13*(48), 57597–57608. https://doi.org/10.1021/acsami.1c17695

Shen, S., Zhang, X., Cheng, X., Xu, Y., Gao, S., Zhao, H., Zhou, X., & Huo, L. (2019). Oxygen-vacancy-enriched porous α-MoO_3 nanosheets for trimethylamine sensing. *ACS Applied Nano Materials*, *2*(12), 8016–8026. https://doi.org/10.1021/acsanm.9b02072

Shen, Z., Zhang, X., Mi, R., Liu, M., Chen, Y., Chen, C., & Ruan, S. (2018). On the high response towards TEA of gas sensors based on Ag-loaded 3D porous ZnO microspheres. *Sensors and Actuators B: Chemical*, *270*, 492–499. https://doi.org/10.1016/j.snb.2018.05.034

Shi, C., Yang, X., Han, S., Fan, B., Zhao, Z., Wu, X., & Qian, J. (2018). Nondestructive prediction of Tilapia fillet freshness during storage at different temperatures by integrating an electronic nose and tongue with radial basis function neural networks. *Food and Bioprocess Technology*, *11*(10), 1840–1852. https://doi.org/10.1007/s11947-018-2148-8

Sovizi, M. R., & Mirzakhani, S. (2020). A chemiresistor sensor modified with lanthanum oxide nanoparticles as a highly sensitive and selective sensor for dimethylamine at room temperature. *New Journal of Chemistry*, *44*(12), 4927–4934. https://doi.org/10.1039/C9NJ06329C

Srinivasan, P., & Rayappan, J. B. B. (2020). Investigations on room temperature dual sensitization of ZnO nanostructures towards fish quality biomarkers. *Sensors and Actuators B: Chemical*, *304*, 127082. https://doi.org/10.1016/j.snb.2019.127082

Srinivasan, P., & Rayappan, J. B. B. (2021). Chemi-resistive sensing of methylamine species using twinned α-MoO_3 nanorods: Role of grain features, activation energy and surface defects. *Sensors and Actuators B: Chemical*, *349*, 130759. https://doi.org/10.1016/j.snb.2021.130759

Tang, X., & Yu, Z. (2020). Rapid evaluation of chicken meat freshness using gas sensor array and signal analysis considering total volatile basic nitrogen. *International Journal of Food Properties*, *23*(1), 297–305. https://doi.org/10.1080/10942912.2020.1716797

Tonezzer, M. (2021a). Detection of Mackerel fish spoilage with a gas sensor based on one single SnO_2 nanowire. *Chemosensors*, *9*(1), 2. https://doi.org/10.3390/chemosensors9010002

Tonezzer, M. (2021b). Single nanowire gas sensor able to distinguish fish and meat and evaluate their degree of freshness. *Chemosensors*, *9*(9), 249. https://doi.org/10.3390/chemosensors9090249

Tonezzer, M., Thai, N. X., Gasperi, F., Van Duy, N., & Biasioli, F. (2021). Quantitative assessment of Trout fish spoilage with a single nanowire gas sensor in a thermal gradient. *Nanomaterials*, *11*(6), 1604. https://doi.org/10.3390/nano11061604

Vajdi, M., Varidi, M. J., Varidi, M., & Mohebbi, M. (2019). Using electronic nose to recognize fish spoilage with an optimum classifier. *Journal of Food Measurement and Characterization*, *13*(2), 1205–1217. https://doi.org/10.1007/s11694-019-00036-4

Verma, P., & Yadava, R. D. S. (2015). Polymer selection for SAW sensor array based electronic noses by fuzzy c-means clustering of partition coefficients: Model studies on detection of freshness and spoilage of milk and fish. *Sensors and Actuators B: Chemical*, *209*, 751–769. https://doi.org/10.1016/j.snb.2014.11.149

Waite, R., & Beveridge, M. (2014). *Improving productivity and environmental performance of aquaculture*. WorldFish. https://www.wri.org/research/improving-productivity-and-environmental-performance-aquaculture

Wang, G., Yang, S., Cao, L., Jin, P., Zeng, X., Zhang, X., & Wei, J. (2021). Engineering mesoporous semiconducting metal oxides from metal-organic frameworks for gas sensing. *Coordination Chemistry Reviews*, *445*, 214086. https://doi.org/10.1016/j.ccr.2021.214086

Wang, M., Gao, F., Wu, Q., Zhang, J., Xue, Y., Wan, H., & Wang, P. (2018). Real-time assessment of food freshness in refrigerators based on a miniaturized electronic nose. *Analytical Methods*, *10*(39), 4741–4749. https://doi.org/10.1039/C8AY01242C

Wang, P., Zheng, Z., Cheng, X., Sui, L., Gao, S., & Zhang, X. (2017). Ionic liquid-assisted synthesis of α-Fe_2O_3 mesoporous nanorod arrays and their excellent trimethylamine gas-sensing properties for monitoring fish freshness. *Journal of Materials Chemistry A*, *5*(37), 19846–19856. https://doi.org/10.1039/C7TA06392J

Wang, W., Zhang, L., Liu, Z., Kang, Y., Chen, Q., & Wang, W. (2022). Visible-light-activated TiO_2–$NiFe_2O_4$ heterojunction for detecting sub-ppm trimethylamine. *Journal of Alloys and Compounds*, *898*, 162990. https://doi.org/10.1016/j.jallcom.2021.162990

Wang, X., Han, W., Yang, J., Cheng, P., Wang, Y., Feng, C., Wang, C., Zhang, H., Sun, Y., & Lu, G. (2022). Conductometric ppb-level triethylamine sensor based on macroporous WO_3-$W_{18}O_{49}$ heterostructures functionalized with carbon layers and PdO nanoparticles. *Sensors and Actuators B: Chemical*, *361*, 131707. https://doi.org/10.1016/j.snb.2022.131707

Wang, X., Li, Y., Li, Z., Zhang, S., Deng, X., Zhao, G., & Xu, X. (2019). Highly sensitive and low working temperature detection of trace triethylamine based on TiO_2 nanoparticles decorated CuO nanosheets sensors. *Sensors and Actuators B: Chemical*, *301*, 127019. https://doi.org/10.1016/j.snb.2019.127019

Wang, Y., Zhang, S., Huang, C., Qu, F., Yao, D., Guo, H., Xu, H., Jiang, C., & Yang, M. (2021). Mesoporous WO_3 modified by Au nanoparticles for enhanced trimethylamine gas sensing properties. *Dalton Transactions*, *50*(3), 970–978. https://doi.org/10.1039/D0DT03131C

Weichselbaum, E., Coe, S., Buttriss, J., & Stanner, S. (2013). Fish in the diet: A review. *Nutrition Bulletin*, *38*(2), 128–177. https://doi.org/10.1111/nbu.12021

Wen, J., Song, Z., Ding, J., Wang, F., Li, H., Xu, J., & Zhang, C. (2022). MXene-derived TiO_2 nanosheets decorated with Ag nanoparticles for highly sensitive detection of ammonia at room temperature. *Journal of Materials Science & Technology*, *114*, 233–239. https://doi.org/10.1016/j.jmst.2021.12.005

Wu, D., Zhang, M., Chen, H., & Bhandari, B. (2021). Freshness monitoring technology of fish products in intelligent packaging. *Critical Reviews in Food Science and Nutrition*, *61*(8), 1279–1292. https://doi.org/10.1080/10408398.2020.1757615

Wu, K., Li, J., & Zhang, C. (2019). Zinc ferrite based gas sensors: A review. *Ceramics International*, *45*(9), 11143–11157. https://doi.org/10.1016/j.ceramint.2019.03.086

Wu, K., Debliquy, M., & Zhang, C. (2022). Room temperature gas sensors based on Ce doped TiO_2 nanocrystals for highly sensitive NH_3 detection. *Chemical Engineering Journal*, *444*, 136449. https://doi.org/10.1016/j.cej.2022.136449

Wu, K., Zhang, W., Zheng, Z., Debliquy, M., & Zhang, C. (2022). Room-temperature gas sensors based on titanium dioxide quantum dots for highly sensitive and selective H2S detection. *Applied Surface Science*, *585*, 152744. https://doi.org/10.1016/j.apsusc.2022.152744

Wu, K.-D., Xu, J.-Y., Debliquy, M., & Zhang, C. (2021). Synthesis and NH_3/TMA sensing properties of $CuFe_2O_4$ hollow microspheres at low working temperature. *Rare Metals*, *40*(7), 1768–1777. https://doi.org/10.1007/s12598-020-01609-9

Wu, L., Pu, H., & Sun, D.-W. (2019). Novel techniques for evaluating freshness quality attributes of fish: A review of recent developments. *Trends in Food Science & Technology*, *83*, 259–273. https://doi.org/10.1016/j.tifs.2018.12.002

Xiong, Y., Liu, W., Qiao, X., Song, X., Wang, S., & Zhang, X. (2021). Confined synthesis of 2D ultrathin ZnO/Co_3O_4 nanomeshes heterostructure for superior triethylamine detection at low temperature. *Sensors and Actuators B: Chemical*, *346*, 130486. https://doi.org/10.1016/j.snb.2021.130486

Xu, H.-Y., Chen, Z.-R., Liu, C.-Y., Ye, Q., Yang, X.-P., Wang, J.-Q., & Cao, B.-Q. (2021). Preparation of {200} crystal faced SnO_2 nanorods with extremely high gas sensitivity at lower temperature. *Rare Metals*, *40*(8), 2004–2016. https://doi.org/10.1007/s12598-021-01720-5

Yan, W., Xu, H., Ling, M., Zhou, S., Qiu, T., Deng, Y., Zhao, Z., & Zhang, E. (2021). MOF-derived porous hollow Co_3O_4@ZnO cages for high-performance MEMS trimethylamine sensors. *ACS Sensors*, *6*(7), 2613–2621. https://doi.org/10.1021/acssensors.1c00315

Yang, J., Han, W., Ma, J., Wang, C., Shimanoe, K., Zhang, S., Sun, Y., Cheng, P., Wang, Y., Zhang, H., & Lu, G. (2021). Sn doping effect on NiO hollow nanofibers based gas sensors about the humidity dependence for triethylamine detection. *Sensors and Actuators B: Chemical*, *340*, 129971. https://doi.org/10.1016/j.snb.2021.129971

Yang, M., Zhang, X., Guo, C., Cheng, X., Zhu, C., Xu, Y., Major, Z., & Huo, L. (2021). Resistive room temperature DMA gas sensor based on the forest-like unusual n-type PANI/TiO_2 nanocomposites. *Sensors and Actuators B: Chemical*, *342*, 130067. https://doi.org/10.1016/j.snb.2021.130067

Yang, M., Cheng, X., Zhang, X., Liu, W., Huang, C., Xu, Y., Gao, S., Zhao, H., & Huo, L. (2019). Preparation of highly crystalline NiO meshed nanowalls via ammonia volatilization liquid deposition for H_2S detection. *Journal of Colloid and Interface Science*, *540*, 39–50. https://doi.org/10.1016/j.jcis.2018.12.106

Yang, S., Liu, Y., Chen, W., Jin, W., Zhou, J., Zhang, H., & Zakharova, G. S. (2016). High sensitivity and good selectivity of ultralong MoO_3 nanobelts for trimethylamine gas. *Sensors and Actuators B: Chemical*, *226*, 478–485. https://doi.org/10.1016/j.snb.2015.12.005

Yang, T., Du, L., Zhai, C., Li, Z., Zhao, Q., Luo, Y., Xing, D.-S., & Zhang, M. (2017). Ultrafast response and recovery trimethylamine sensor based on α-Fe_2O_3 snowflake-like hierarchical architectures. *Journal of Alloys and Compounds*, *718*, 396–404. https://doi.org/10.1016/j.jallcom.2017.05.227

Yang, T., Yang, X., Zhu, M., Zhao, H., & Zhang, M. (2020). Coral-like $ZnFe_2O_4$–ZnO mesoporous heterojunction architectures: Synthesis and enhanced sensing properties for triethylamine. *Inorganic Chemistry Frontiers*, *7*(9), 1918–1926. https://doi.org/10.1039/D0QI00134A

Yang, W., Feng, L., He, S., Liu, L., & Liu, S. (2018). Density gradient strategy for preparation of broken In_2O_3 microtubes with remarkably selective detection of triethylamine vapor. *ACS Applied Materials & Interfaces*, *10*(32), 27131–27140. https://doi.org/10.1021/acsami.8b09375

Yuan, H., Li, N., Fan, W., Cai, H., & Zhao, D. (2022). Metal-organic framework based gas sensors. *Advanced Science*, *9*(6), 2104374. https://doi.org/10.1002/advs.202104374

Yuan, Z., Bariya, M., Fahad, H. M., Wu, J., Han, R., Gupta, N., & Javey, A. (2020). Trace-level, multi-gas detection for food quality assessment based on decorated silicon transistor arrays. *Advanced Materials*, *32*(21), 1908385. https://doi.org/10.1002/adma.201908385

Zambotti, G., Soprani, M., Gobbi, E., Capuano, R., Pasqualetti, V., Di Natale, C., & Ponzoni, A. (2019). *Early detection of fish degradation by electronic nose*. Presented at the 2019 IEEE International Symposium on Olfaction and Electronic Nose (ISOEN). https://doi.org/10.1109/ISOEN.2019.8823461

Zambotti, G., Soprani, M., Gobbi, E., Capuano, R., Pasqualetti, V., Di Natale, C., & Ponzoni, A. (2020). Portable electronic nose device for the identification of food degradation. In G. Di Francia, C. Di Natale, B. Alfano, S. De Vito, E. Esposito, G. Fattoruso, F. Formisano, E. Massera, M. L. Miglietta, & T. Polichetti (Eds.), *Sensors and microsystems* (pp. 91–95). Springer International Publishing. https://doi.org/10.1007/978-3-030-37558-4_14

Zaukuu, J. L. Z., Bazar, G., Gillay, Z., & Kovacs, Z. (2020). Emerging trends of advanced sensor based instruments for meat, poultry and fish quality – A review. *Critical Reviews in Food Science and Nutrition*, *60*(20), 3443–3460. https://doi.org/10.1080/10408398.2019.1691972

Zhang, C., Huan, Y., Li, Y., Luo, Y., & Debliquy, M. (2022). Low concentration isopropanol gas sensing properties of Ag nanoparticles decorated In_2O_3 hollow spheres. *Journal of Advanced Ceramics*, *11*(3), 379–391. https://doi.org/10.1007/s40145-021-0530-x

Zhang, C., Li, Y., Liu, G.-F., & Liao, H.-L. (2022). Preparation of ZnO_{1-x} by peroxide thermal decomposition and its room temperature gas sensing properties. *Rare Metals*, *41*(3), 871–876. https://doi.org/10.1007/s12598-021-01840-y

Zhang, C., Wu, K., Liao, H., & Debliquy, M. (2022). Room temperature WO_3-Bi_2WO_6 sensors based on hierarchical microflowers for ppb-level H_2S detection. *Chemical Engineering Journal*, *430*, 132813. https://doi.org/10.1016/j.cej.2021.132813

Zhang, D., Yu, S., Wang, X., Huang, J., Pan, W., Zhang, J., Meteku, B. E., & Zeng, J. (2022). UV illumination-enhanced ultrasensitive ammonia gas sensor based on (001)TiO_2/MXene heterostructure for food spoilage detection. *Journal of Hazardous Materials*, *423*, 127160. https://doi.org/10.1016/j.jhazmat.2021.127160

Zhang, F., Dong, X., Cheng, X., Xu, Y., Zhang, X., & Huo, L. (2019). Enhanced gas-sensing properties for trimethylamine at low temperature based on MoO_3/$Bi_2Mo_3O_{12}$ hollow microspheres. *ACS Applied Materials & Interfaces*, *11*(12), 11755–11762. https://doi.org/10.1021/acsami.8b22132

Zhang, F., Zheng, M., Zhang, X., Cheng, X., Li, M., Huo, L., Zhou, X., & Xu, Y. (2022). Rapid detection of H_2S gas driven by the catalysis of flower-like α-$Bi_2Mo_3O_{12}$ and its visual performance: A combined experimental and theoretical study. *Journal of Hazardous Materials*, *424*, 127734. https://doi.org/10.1016/j.jhazmat.2021.127734

Zhang, S., Song, P., Tian, Z., & Wang, Q. (2018). Synthesis of mesoporous In_2O_3 nanocubes and their superior trimethylamine sensing properties. *Materials Science in Semiconductor Processing*, *75*, 58–64. https://doi.org/10.1016/j.mssp.2017.11.029

Zhang, Z., Zhang, S., Jiang, C., Guo, H., Qu, F., Shimakawa, Y., & Yang, M. (2021). Integrated sensing array of the perovskite-type $LnFeO_3$ (Ln = La, Pr, Nd, Sm) to discriminate detection of volatile sulfur compounds. *Journal of Hazardous Materials*, *413*, 125380. https://doi.org/10.1016/j.jhazmat.2021.125380

Zhao, C., Shen, J., Xu, S., Wei, J., Liu, H., Xie, S., Pan, Y., Zhao, Y., & Zhu, Y. (2022). Ultra-efficient trimethylamine gas sensor based on Au nanoparticles sensitized WO_3 nanosheets for rapid assessment of seafood freshness. *Food Chemistry*, *392*, 133318. https://doi.org/10.1016/j.foodchem.2022.133318

Zhao, Y., Yuan, X., Sun, Y., Wang, Q., Xia, X.-Y., & Tang, B. (2020). Facile synthesis of tortoise shell-like porous $NiCo_2O_4$ nanoplate with promising triethylamine gas sensing properties. *Sensors and Actuators B: Chemical*, *323*, 128663. https://doi.org/10.1016/j.snb.2020.128663

Zhou, L., Mi, Q., Jin, Y., Li, T., & Zhang, D. (2021). Construction of MoO_3/$MoSe_2$ nanocomposite-based gas sensor for low detection limit trimethylamine sensing at room temperature. *Journal of Materials Science: Materials in Electronics*, *32*(13), 17301–17310. https://doi.org/10.1007/s10854-021-06242-5

Zhou, Q., Xu, L., Kan, Z., Yang, L., Chang, Z., Dong, B., Bai, X., Lu, G., & Song, H. (2022). A multi-platform sensor for selective and sensitive H_2S monitoring: Three-dimensional macroporous ZnO encapsulated by MOFs with small Pt nanoparticles. *Journal of Hazardous Materials*, *426*, 128075. https://doi.org/10.1016/j.jhazmat.2021.128075

Zhu, X., Chang, X., Tang, S., Chen, X., Gao, W., Niu, S., Li, J., Jiang, Y., & Sun, S. (2022). Humidity-tolerant chemiresistive gas sensors based on hydrophobic CeO_2/SnO_2 heterostructure films. *ACS Applied Materials & Interfaces*, *14*(22), 25680–25692. https://doi.org/10.1021/acsami.2c03575

Zhuang, S., Hong, H., Zhang, L., & Luo, Y. (2021). Spoilage-related microbiota in fish and crustaceans during storage: Research progress and future trends. *Comprehensive Reviews in Food Science and Food Safety*, *20*(1), 252–288. https://doi.org/10.1111/1541-4337.12659

How to cite this article: Wu, K., Debliquy, M., & Zhang, C. (2022). Metal–oxide–semiconductor resistive gas sensors for fish freshness detection. *Comprehensive Reviews in Food Science and Food Safety*, 1–33. https://doi.org/10.1111/1541-4337.13095